

UNITED STATES DEPARTMENT OF THE INTERIOR  
GEOLOGICAL SURVEY

Mapping of an Aquifer Boundary near Kunia, O'ahu, Hawai'i  
using Schlumberger Soundings

by

Jim Kauahikaua and Dallas B. Jackson

Open-File Report 88-228

This report is preliminary and has not been reviewed for conformity with U.S.  
Geological Survey editorial standards and stratigraphic nomenclature.

1988

## Abstract

Schlumberger soundings were used to determine the depth to a layer of clay-rich, weathered volcanics between the older Wai'anae lava series and the younger Ko'olau lava series on O'ahu, Hawai'i. The location at which this layer intersects the water table at sea level is of local hydrologic significance because the layer appears to act as an aquiclude separating fresh water within the Ko'olau lavas to the east from brackish water within the Wai'anae lavas to the west. From a profile of soundings at the 122 meter (400 feet) elevation, we were able to trace a low-resistivity layer dipping eastward which is thought to be the target layer. The interpolated intersection of this low-resistivity layer with sea level was later drilled; a 25-m thick layer of clay and weathered volcanics was found at sea level.

## Introduction

Growing demands on the ground-water resources of Central O'ahu from increased population and agriculture require better understanding of the resource dimensions. Detailed mapping of aquifer boundaries, such as those of the Schofield high-level aquifer (Kauahikaua and Shettigara, 1984), allow more accurate water budget calculations to be made. This report describes mapping of another ground-water boundary in south central O'ahu between the towns of Kunia and Waipahu using Schlumberger soundings. Wells developing ground water in Wai'anae lava aquifers (ground-water area 11) have hydraulic heads that are about 0.5 m lower than adjacent wells developing water in Ko'olau lava aquifers (ground-water area 6; Visher and Mink, 1964). The ground water in the Wai'anae aquifer is also slightly more brackish than that in the Ko'olau aquifer (C. Hunt, oral communication, 1985). Although it has never been explicitly identified, the barrier between these two aquifers is thought to be a layer of soil and alluvium representing an erosional unconformity between the Wai'anae and Ko'olau lavas (described north of the Leilehua plateau by Stearns and Vaksvik, 1935). The unconformity is not vertical but probably dips gently eastward mantling the Wai'anae flows.

If this unconformity is the aquifer barrier, then electrical geophysical techniques might be able to trace it below the surface. The unconformity should be a good electrical target because it consists of low-resistivity clayey soil and is electrically quite different from the unweathered rocks above and below it which have high resistivity. The aquifer boundary could then be placed where the unconformity intersected the water table. Previous work in central O'ahu (Kauahikaua and Shettigara, 1984) demonstrated that a set of Schlumberger soundings could resolve this layer at least to depths of a few hundred meters. To illustrate the resolution of the Schlumberger technique for this type of problem, several theoretical model curves were computed for models with shallow structure similar to that expected in Kunia<sup>1</sup>, but with a thin, low-resistivity layer (representing the soil and alluvium at the unconformity) inserted at various depths within the deeper, resistive unit representing unweathered lavas. Figure 1 shows six curves for models with the thin layer placed at progressively greater depths. The curves shown are purposely incomplete and were calculated to an electrode spacing of 1000 m only - the maximum electrode spacing that was intended for field work. Note the approximately 45° line of increasing apparent resistivity with increasing electrode spacing present in all curves. Each curve drops below this line at

<sup>1</sup> 15 m of 12 ohm-m material representing surface soils and weathering products over 340 ohm-m unweathered basalt

an electrode spacing which is approximately equal to the depth at which the thin layer has been placed. It is clear that electrode spacings equal to at least two times the depth to the thin layer are required for resolution of the depth to the top of the thin layer.

Because the barrier, or target, layer is thin with respect to its depth of burial, we do not expect to be able to separately resolve the layer's thickness and resistivity. Instead, we can resolve its "conductance" which is the layer's thickness divided by its resistivity. Figure 2 shows four model curves in which the depth of burial is kept constant, but the conductance is varied. Clearly, the larger the conductance of such a layer (e.g. the thicker the layer or the lower its resistivity), the more "visible" (i.e. the more sharply that curve departs from the 45° line) it would be on a Schlumberger sounding; however, the electrode spacing at which the curves initially depart from the 45° slope is almost identical in each of the curves. These model studies show that the detectability of a thin, low-resistivity layer is enhanced by having a large conductance.

### Field Procedures

During four days of field work in October 1985, ten Schlumberger soundings were obtained in the area bounded by Kunia Road and the H-1 freeway. Of the nine successful soundings, six were located along an east-west profile at an elevation of 122 meters (400 feet) and three were located at an elevation of 213 meters (700 feet). Details of the operation and interpretation of the soundings are in Appendix A. Sounding locations are shown in Figure 3.

### Results of Schlumberger sounding at Kunia, O'ahu

All soundings showed a generally increasing resistivity with depth. Specific interpretations detail a sequence of low to moderate resistivities from the surface to the top of a thick layer assigned a resistivity of 340 ohm-m. These surficial layers probably represent soil and alluvium. The total thickness of these surficial layers ranges between 8.7 to 18.1 m for the soundings obtained at the 122 m elevation and 22.1 to 34 m for the soundings at about 213 m elevation. Sounding 6, located in Honouliuli gulch, is an exception with over 62 m of surficial material above the more resistive layer;

we believe that this reflects the geoelectric structure of the deep gulch rather than that of the plain dissected by the gulch. In general, the trend of thicker surficial layers at higher elevations is confirmed by previous soundings which show interpreted surface layer thicknesses of more than 70 m at elevations above 244 m on the Leilehua (Schofield) plateau (Kauahikaua and Shettigara, 1984).

The bulk of the section interpreted from each set of sounding data is a single layer assigned a resistivity of 340 ohm-m. It is assigned rather than interpreted because, in most soundings, that particular resistivity is not well determined by the data. That value is only determined well by soundings 4 and 8 to be about 341 and 362 ohm-m, respectively; therefore, the corresponding layer in the other soundings was assigned 340 ohm-m. This assigned value also agrees with that interpreted from soundings just to the north by Kauahikaua and Shettigara (1984). In that study, as well as in the present one, the 340 ohm-m layer is interpreted to represent unweathered lavas.

The presence of a thin, conductive layer at increasingly greater depths in soundings farther to the east is clear in the data plot of Figure 4. The apparent resistivities depart from the approximately 45° slope at increasingly larger electrode spacings as one goes east, just as predicted by the model plots shown in Figure 1. The greater variation in the curves in Figure 4 compared to Figure 1 is due primarily to variations in the surface layer of conductive soil. Figure 5 summarizes the interpretation of soundings 7, 1, 6, 5, 4, and 8 along an approximately east-west profile at an approximately-constant elevation of 122 m. The target interface can be seen clearly in soundings 5, 4, and 8 on the east end of that profile. The layer dips eastward and passes through sea level about midway between soundings 5 and 4. Sounding 6, located within Honouliuli gulch, seems to be no more than 10 m above the conductive layer and soundings 7 and 1 do not show evidence of the target layer below the surficial conductive layer. Both soundings require lower resistivities near sea level; however, that part of the section is poorly determined by the sounding data and is considered more indicative of the water table. The conductive layer (of 41 ohm-m) in soundings 6 may be thick due to accumulation of weathering products in the deep gulch.

Figure 6 summarizes the interpretive results of soundings 2, 9 and 10 at an elevation of approximately 213 m. The interpretation of sounding 2 suggests a conductor beneath the 340 ohm-m layer at about 230 m below sea level. Again, this is not well determined by the data and is highly questionable. The decrease in resistivity beneath the locations of soundings 9 and 10 is believed to indicate the target layer, again dipping to the east; the layer intersects sea level just to the west of sounding 9.

As expected, the resolution of the properties of the target layer is generally poor. The resistivity of the target layer is interpreted to be 40 to 59 (some 40 ohm-m values are assigned because the inversion process interpreted unrealistically low resistivities for this unit). Its thickness is not resolved at all as it always forms the last layer in each sounding in which it is detected. The only parameter determined by the data for this

layer is the depth to its top. This was expected because the survey was designed this way - the general geoelectric section to be encountered was already well known from Kauahikaua and Shettigara (1984) so that, during this survey, soundings were only carried out until the first signs of a conductor were seen clearly in the field data. Shorter soundings allowed more soundings to be obtained in the allotted field time and provided an optimally low-cost survey. The questions of thickness and/or resistivity of the interface were not important; therefore, no field time was spent determining those values.

### Comparison of the Schlumberger results with 1900 drilling results

In late summer 1986, two wells were drilled between soundings 4 and 5 at an elevation of about 122 m. They encountered a layer of red clay and ash at 115.5 m and drilled through it into unweathered basalt at a depth of 140.2 m. The layer has been identified as the unconformity between Ko'olau and Wai'anae lavas (C. Hunt, 1986, oral communication). The Schlumberger results also place the intersection of the thin conductive layer and sea level between soundings 4 and 5. The drilling results confirm our interpretation that the thin, electrically-conductive layer seen in many of the Schlumberger soundings is the unconformity between Wai'anae and Ko'olau lavas.

### Conclusions and Recommendations

On the central plateau of O'ahu, short-spacing Schlumberger soundings are an effective tool for determining the depth to a thin conductive interface within more resistive material if that depth is no more than 200 m. Although one sounding in this study is interpreted to have resolved the conductive layer at almost 500 m below the surface, we feel that it is an exception.

A conductive layer was successfully traced eastward from the Wai'anae mountains that corresponded to an unconformity between Wai'anae and Ko'olau lavas. The unconformity is electrically conductive because it is probably represented by soil and alluvium. Figure 7 shows the location of the interpolated intersection of the interpreted unconformity and sea level. That intersection is our best estimate of the boundary between the Wai'anae and Ko'olau aquifers in this area.

## APPENDIX A: Schlumberger Sounding Data and Computer Interpretations

A resistivity sounding consists of a series of apparent resistivity measurements taken at several different electrode positions created by expanding four electrodes symmetrically about a central point (two on each side), preferably along a straight line. Electric current is forced into the ground through the outer two electrodes (current electrodes) and the voltage produced by that current is measured between the inner two electrodes (potential electrodes). Larger current electrode separations generally force deeper current penetration; thus, it is possible to influence the depth of investigation by varying the current electrode separation. For the Schlumberger electrode array, the potential electrodes are placed no farther apart than one-fifth the separation between the current electrodes.

Effects of lateral inhomogeneities can sometimes be recognized by moving either the potential electrodes or the current electrodes between readings, but not both at the same time. In practice, the distance between potential electrodes is expanded once for every four or five current electrode expansions. Apparent resistivity values obtained for the same current electrode separation with two different potential electrode separations are almost always slightly different due to small inhomogeneities around the electrodes and/or the use of homogeneous earth potential variations to reduce real, nonhomogeneous earth potential variations; this difference must be removed to give an unbroken data set for quantitative interpretation. The differences are removed by holding a data segment, made with a particular potential electrode separation, fixed and shifting the remaining segments up or down so that the end points match adjacent segments. A common convention is to shift all segments to the segment measured with the largest potential electrode spacing.

Computer program MARQDCLAGT, an enhanced version of MARQDCLAG (Anderson, 1979) written in Rocky Mountain BASIC 4.0, offers an automatic means by which sounding data sets, like those obtained in the course of this study, can be inverted to their best-fitting horizontally-layered model parameters - resistivities and thickness. The layers in the model may either have a uniform resistivity or a resistivity which varies from the resistivity of the layer above it to the resistivity of the layer below. The resistivity can be selected to vary linearly in either resistivity or conductivity. Of course, approximate matching can be done by manually comparing the sounding data to theoretical curves in a standard album; however, the computer inversion offers several advantages, including speed, automation, and estimation of parameter resolution.

MARQDCLAGT automatically minimizes the following quantity:

$$\text{PHI} = \sum_{i=1}^N \left[ \frac{y_i - f(x_i)}{e_i} \right]^2 \quad (\text{A.1})$$

where N is the number of data points in the sounding data set,

$x_i$  is the  $i^{\text{th}}$  current electrode spacing,

$y_i$  is the measured apparent resistivity at  $x_i$ ,

$e_i$  is the apparent-resistivity measurement error

(default =  $y_i/100$  or 1%), and

$f(x_i)$  is the theoretical apparent resistivity calculated from the earth model at  $x_i$ .

Along with the sounding data set, the program requires a starting guess of all model parameters.

The number of layers cannot be automatically varied by the program so it is a common practice to invert each sounding data set for several models, each having a different number of layers. The best-fitting model is chosen to be the one which minimizes the following quantity, called the reduced chi-squared statistic:

$$\text{REDUCED CHI-SQUARED} = \text{PHI} / (N - 1 - K) \quad (\text{A.2})$$

where K is the number of parameters in the model being fit to the data and PHI is defined in equation (A.1). In general applications,  $K = 2 * m - 1$  where m is the number of layers in the theoretical model and \* denotes multiplication.

During the inversions of the sounding data sets, the natural logarithm of the model parameters, rather than the parameters themselves, were manipulated to avoid the possibility of negative resistivities or thicknesses and to more accurately reflect the logarithmic resolution of these values. The values and their error estimates are converted back to normal units before being output by the program. A detailed description of the headings and identifying terms used in the program output listed in this Appendix follows:

X                      electrode spacing equal to half the distance between the two current electrodes, meters,

OBSERVED              shifted observed apparent resistivity values, ohm-meters,



PREDICTED            apparent resistivity values predicted or calculated from the best-fitting model parameters,

%RESIDUALS             $(\text{OBSERVED} - \text{PREDICTED}) * 100$ ,

WEIGHT FN             $1/(\text{error})^2$ , where error is normally  $\text{OBSERVED}/100$ ,

CORRELATION MATRIX estimates of the correlation between each of the model parameters and any other parameters of this particular model. Values of one down the matrix diagonal indicate that each parameter is 100% positively correlated with itself (as expected). Numbers between +1 and -1 off the diagonal indicate the degree of correlation between each pair of parameters. A correlation of zero indicates no correlation. A correlation of +1 or -1 indicate perfect positive or negative correlation, respectively. The integer numbers labeling the rows and columns of the matrix are parameter numbers. If the model has m layers then parameters 1 through m correspond to resistivities for layers 1 through m and parameters m+1 through 2\*m-1 correspond to thicknesses for layers 1 through m-1.

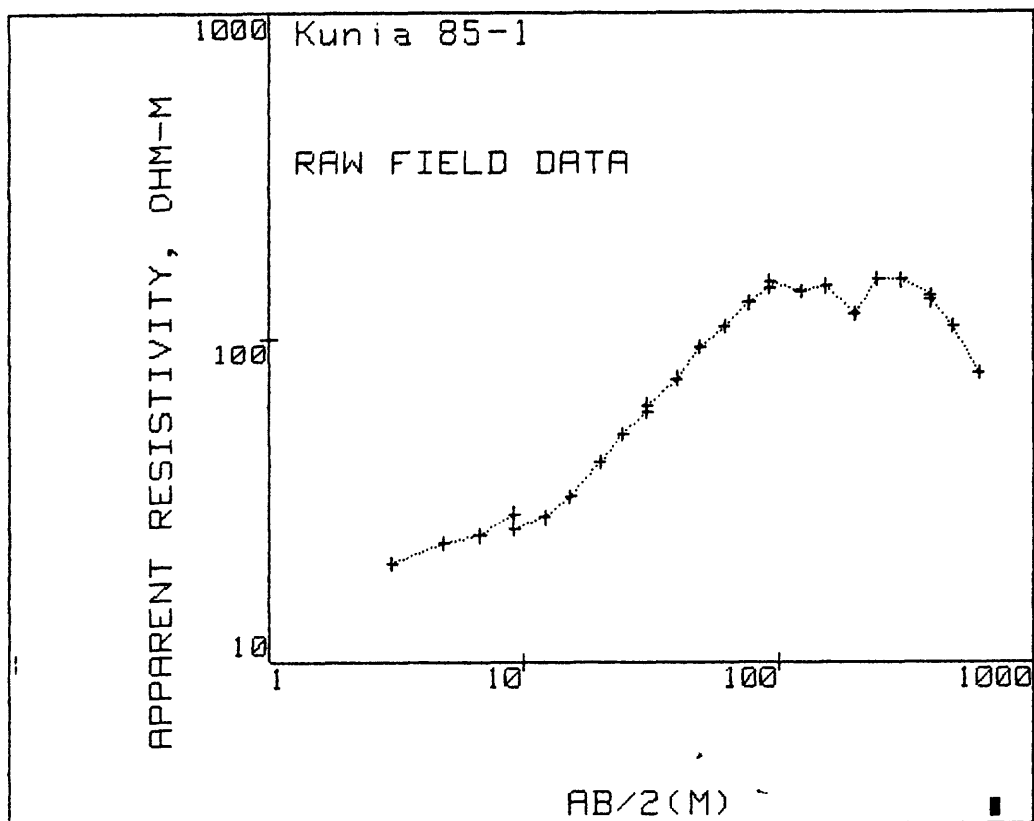
REDUCED CHI-SQUARED    the statistic defined in equation (A.2),

RESISTIVITY            in ohm-m, three columns with the left- and right-most column indicating lower and upper estimated bounds on the best-fitting resistivity in the middle column. Asterisks indicate that resistivity was not allowed to vary during the inversion. Blanks in the right-most column indicate an upper bound that is essentially infinite (no upper bound). Negative resistivities indicate transitional layers. A resistivity of -1 indicates a linear resistivity and -2 indicates a linear conductivity.

THICKNESS            in meters, three columns with the left- and right-most column indicating lower and upper estimated bounds on the best-fitting thickness in the middle column. Asterisks indicate that thickness was not allowed to vary during the inversion. Blanks in the right-most column indicate an upper bound that is essentially infinite (no upper bound).

DEPTH            in meters, depth to the upper surface of that layer from ground surface.

ELEV            in meters, elevation of the upper surface of that layer from sea level if the sounding elevation has been entered, or from ground surface (in this case  $\text{ELEV} = - \text{DEPTH}$ ).



AB/2 (M) APP.RHO

3.0	20.0
4.9	23.3
6.7	24.4
9.1	28.5
9.1	25.6
12.2	27.8
15.2	32.2
19.8	41.1
24.4	50.4
30.5	59.0
30.5	62.2
39.6	75.0
48.8	94.0
61.0	108.0
76.2	128.0
91.4	142.0
91.4	149.0
121.9	138.0
152.4	144.0
198.1	118.0
243.8	151.0
304.8	150.0
396.2	135.0
396.2	130.0
487.7	108.0
609.6	78.0

## MARQUARDT STATISTICS: Kunia 85-1

	X	OBSERVED	PREDICTED	%RESIDUALS	WEIGHT FN
1	+3.0480E+00	+1.9137E+01	+1.9389E+01	-1.3174E+00	+5.0775E+00
2	+4.8768E+00	+2.2247E+01	+2.1649E+01	+2.6857E+00	+3.7572E+00
3	+6.7056E+00	+2.3347E+01	+2.3525E+01	-7.6262E-01	+3.4114E+00
4	+9.1440E+00	+2.7270E+01	+2.6370E+01	+3.2993E+00	+2.5005E+00
5	+1.2192E+01	+2.9614E+01	+3.0770E+01	-3.9051E+00	+2.1204E+00
6	+1.5240E+01	+3.4301E+01	+3.5878E+01	-4.5979E+00	+1.5805E+00
7	+1.9812E+01	+4.3781E+01	+4.4128E+01	-7.9309E-01	+9.7010E-01
8	+2.4384E+01	+5.3688E+01	+5.2439E+01	+2.3267E+00	+6.4512E-01
9	+3.0480E+01	+6.2849E+01	+6.3095E+01	-3.9134E-01	+4.7076E-01
10	+3.9624E+01	+7.5782E+01	+7.7856E+01	-2.7361E+00	+3.2378E-01
11	+4.8768E+01	+9.4981E+01	+9.1165E+01	+4.0176E+00	+2.0612E-01
12	+6.0960E+01	+1.0913E+02	+1.0683E+02	+2.1003E+00	+1.5615E-01
13	+7.6200E+01	+1.2934E+02	+1.2341E+02	+4.5829E+00	+1.1116E-01
14	+9.1440E+01	+1.4348E+02	+1.3698E+02	+4.5323E+00	+9.0323E-04
15	+1.2192E+02	+1.3289E+02	+1.5636E+02	-1.7658E+01	+1.0530E-03
16	+1.5240E+02	+1.3867E+02	+1.6719E+02	-2.0572E+01	+9.6705E-04
17	+1.9812E+02	+1.1363E+02	+1.7163E+02	-5.1048E+01	+1.4402E-03
18	+2.4384E+02	+1.4541E+02	+1.6669E+02	-1.4639E+01	+8.7946E-04
19	+3.0480E+02	+1.4444E+02	+1.5246E+02	-5.5479E+00	+8.9123E-02
20	+3.9624E+02	+1.3000E+02	+1.2643E+02	+2.7487E+00	+1.1003E-01
21	+4.8768E+02	+1.0800E+02	+1.0297E+02	+4.6570E+00	+1.5942E-01
22	+6.0960E+02	+7.8000E+01	+8.0011E+01	-2.5783E+00	+3.0563E-01

## CORRELATION MATRIX:

	2	4	5	6	7
2	+1.00	-.07	+.88	+.75	+.05
4	-.07	+1.00	-.05	-.14	-.95
5	+.88	-.05	+1.00	+.43	+.04
6	+.75	-.14	+.43	+1.00	+.10
7	+.05	-.95	+.04	+.10	+1.00

REDUCED CHI-SQUARED=13.4

PHI=214.47

DCLAG: \*\*\*\*\* END \*\*\*\*\*

Kunia 85-1

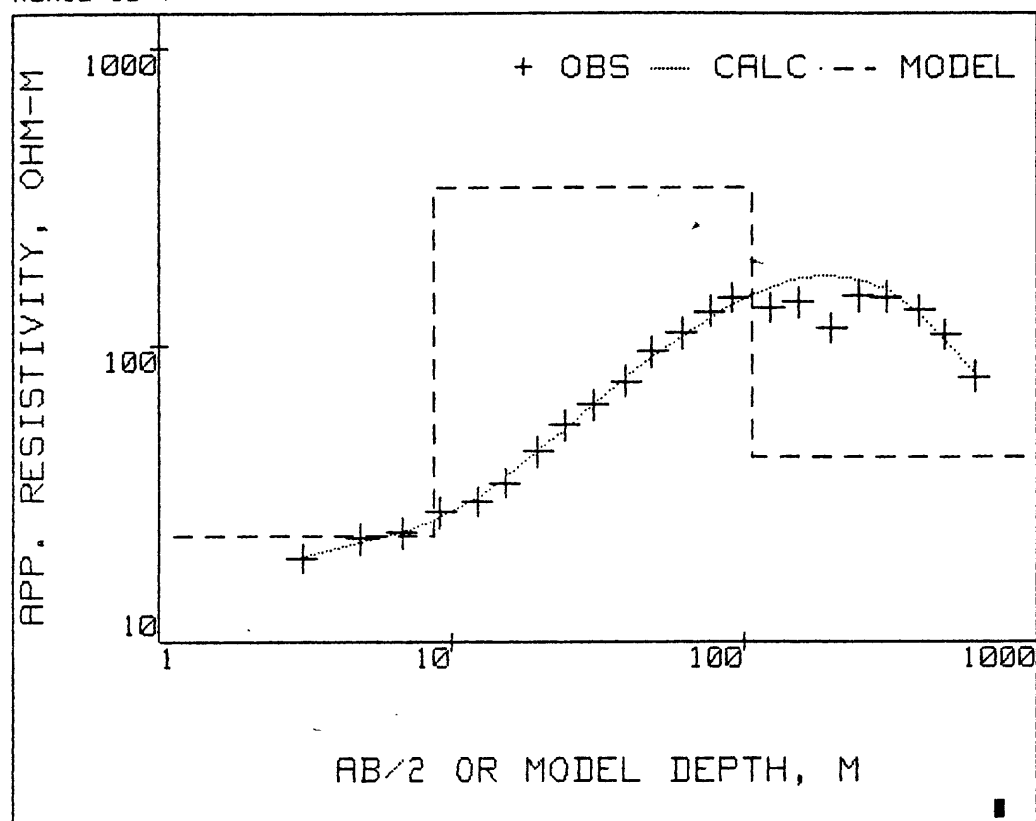
COORDINATES: 0 0

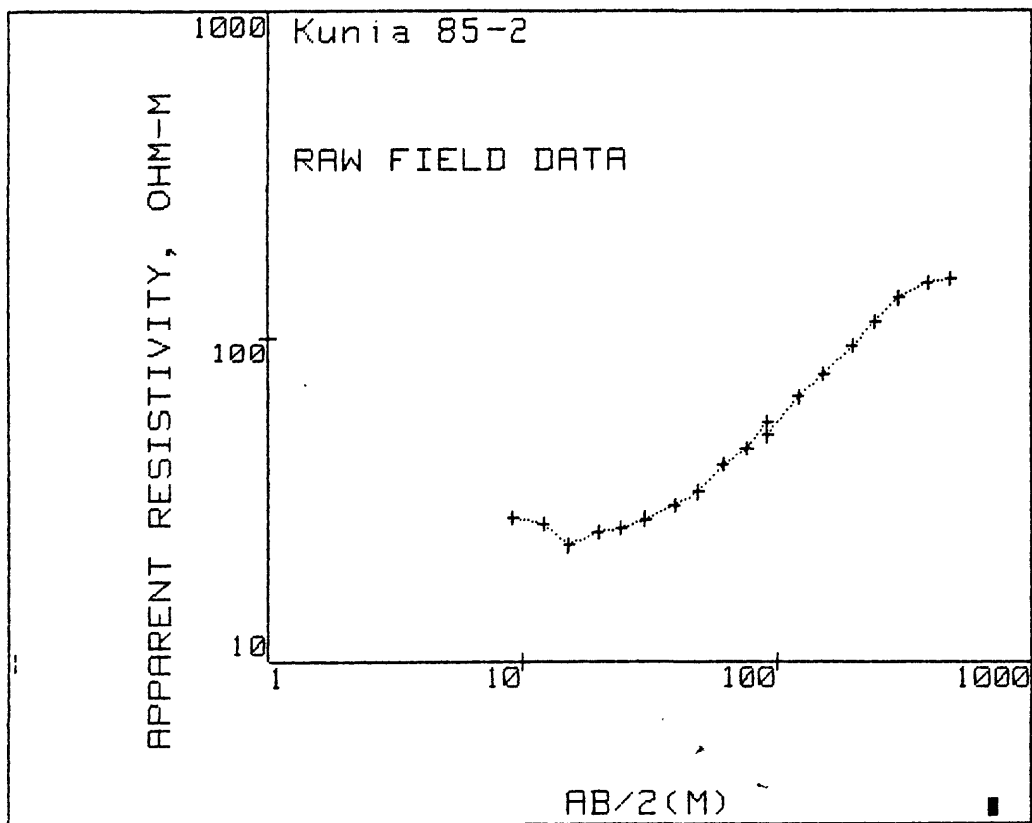
ELEVATION : 116 METER

AZIMUTH :

RESISTIVITY			THICKNESS			DEPTH	ELEV
*****	12.0*****		.3	.6	1.2	0.0	116.0
19.7	22.8	26.4	7.2	8.0	8.9	.6	115.4
*****	340.0*****		82.2	97.2	114.9	8.7	107.3
29.8	42.2	59.6				105.8	10.2

Kunia 85-1





AB/2 (M) APP. RHO

9.1	27.5
12.2	26.4
15.2	22.7
19.8	24.9
24.4	25.6
30.5	27.3
30.5	27.3
39.6	30.1
48.8	33.0
61.0	40.2
76.2	44.9
91.4	54.0
91.4	49.5
121.9	65.0
152.4	77.0
198.1	94.0
243.8	112.0
304.8	132.0
396.2	147.0
487.7	151.0

## MARQUARDT STATISTICS: Kunia 85-2

	X	OBSERVED	PREDICTED	%RESIDUALS	WEIGHT FN
1	+9.1440E+00	+2.5208E+01	+2.5267E+01	-2.3279E-01	+2.0946E+00
2	+1.2192E+01	+2.4200E+01	+2.4037E+01	+6.7531E-01	+2.2728E+00
3	+1.5240E+01	+2.0808E+01	+2.3339E+01	-1.2161E+01	+3.0740E-02
4	+1.9812E+01	+2.2825E+01	+2.3080E+01	-1.1178E+00	+2.5548E+00
5	+2.4384E+01	+2.3467E+01	+2.3461E+01	+2.5309E-02	+2.4170E+00
6	+3.0480E+01	+2.5025E+01	+2.4626E+01	+1.5932E+00	+2.1254E+00
7	+3.9624E+01	+2.7592E+01	+2.7349E+01	+8.8027E-01	+1.7484E+00
8	+4.8768E+01	+3.0250E+01	+3.0860E+01	-2.0166E+00	+1.4546E+00
9	+6.0960E+01	+3.6850E+01	+3.6237E+01	+1.6628E+00	+9.8019E-01
10	+7.6200E+01	+4.1158E+01	+4.3398E+01	-5.4417E+00	+7.8572E-01
11	+9.1440E+01	+4.9500E+01	+5.0573E+01	-2.1678E+00	+5.4322E-01
12	+1.2192E+02	+6.5000E+01	+6.4264E+01	+1.1329E+00	+3.1503E-01
13	+1.5240E+02	+7.7000E+01	+7.6848E+01	+1.9722E-01	+2.2449E-01
14	+1.9812E+02	+9.4000E+01	+9.3727E+01	+2.9047E-01	+1.5064E-01
15	+2.4384E+02	+1.1200E+02	+1.0842E+02	+3.1983E+00	+1.0611E-01
16	+3.0480E+02	+1.3200E+02	+1.2494E+02	+5.3451E+00	+7.6390E-02
17	+3.9624E+02	+1.4700E+02	+1.4395E+02	+2.0723E+00	+6.1596E-02
18	+4.8768E+02	+1.5100E+02	+1.5700E+02	-3.9760E+00	+5.8376E-02

## CORRELATION MATRIX:

	1	3	6	7	8	9
1	+1.00	-.69	-.96	-.85	+.96	-.11
3	-.69	+1.00	+.84	+.95	-.82	+.27
6	-.96	+.84	+1.00	+.96	-1.00	+.16
7	-.85	+.95	+.96	+1.00	-.96	+.20
8	+.96	-.82	-1.00	-.96	+1.00	-.13
9	-.11	+.27	+.16	+.20	-.13	+1.00

REDUCED CHI-SQUARED=9.819

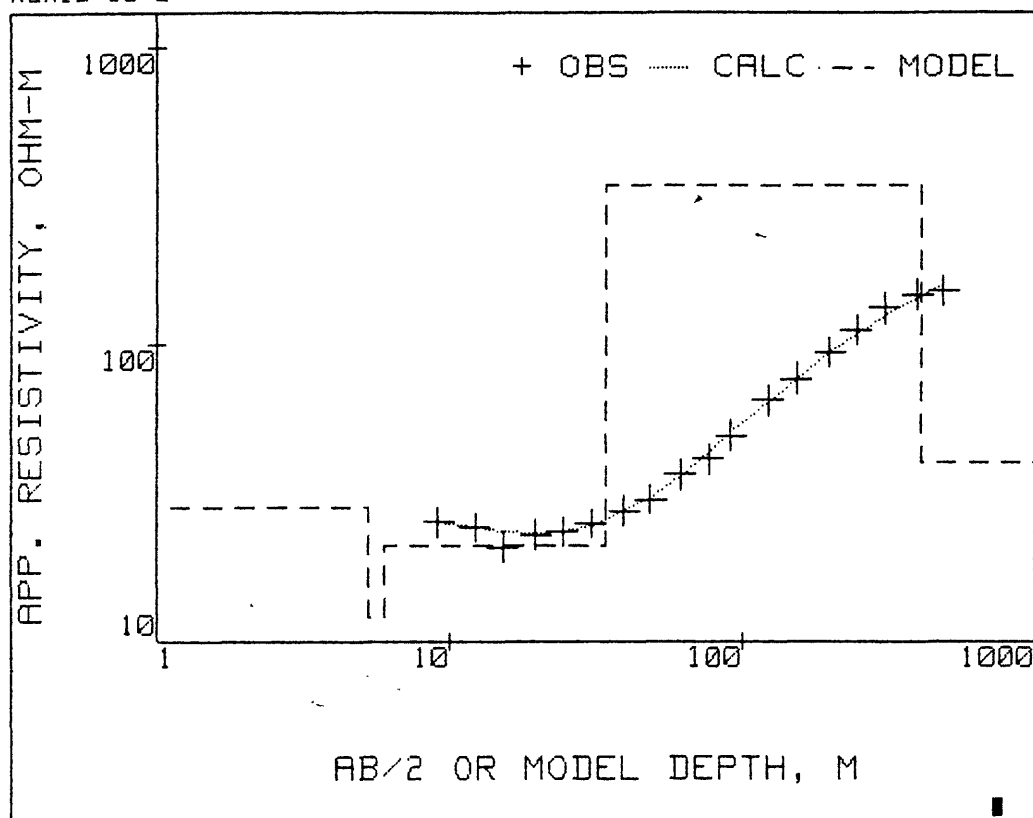
PHI=108

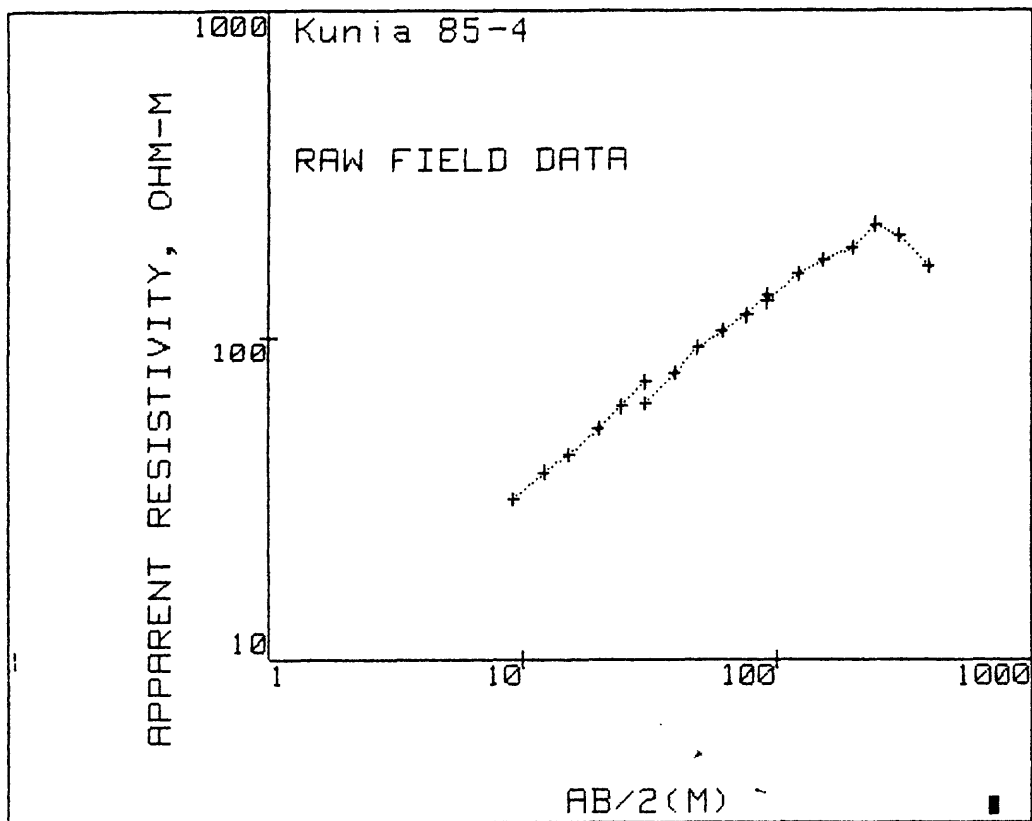
DCLAG: \*\*\*\*\* END \*\*\*\*\*  
 COORDINATES: 0 0  
 ELEVATION : 171 METER  
 AZIMUTH :

Kunia 85-2

RESISTIVITY			THICKNESS			DEPTH	ELEV
9.5	28.4	85.2	0.0	5.2	2494.3	0.0	171.0
*****	12.0*****		0.0	.7		5.2	165.8
12.7	21.0	34.9	5.5	28.1	143.9	5.9	165.1
*****	340.0*****		237.7	372.9	584.8	34.0	137.0
*****	40.0*****					406.9	-235.9

Kunia 85-2





AB/2(M) APP.RHO

9.1	31.3
12.2	38.0
15.2	43.0
19.8	52.0
24.4	60.6
30.5	72.0
30.5	62.0
39.6	77.0
48.8	92.0
61.0	104.0
76.2	116.0
91.4	134.0
91.4	128.0
121.9	156.0
152.4	172.0
198.1	188.0
243.8	221.0
304.8	205.0
396.2	165.0



## MARQUARDT STATISTICS: Kunia 85-4

	X	OBSERVED	PREDICTED	%RESIDUALS	WEIGHT FN
1	+9.1440E+00	+2.5746E+01	+2.5748E+01	-6.5659E-03	+4.8719E+00
2	+1.2192E+01	+3.1257E+01	+3.0968E+01	+9.2330E-01	+3.3054E+00
3	+1.5240E+01	+3.5370E+01	+3.5835E+01	-1.3154E+00	+2.5814E+00
4	+1.9812E+01	+4.2773E+01	+4.2880E+01	-2.5070E-01	+1.7652E+00
5	+2.4384E+01	+4.9847E+01	+4.9832E+01	+2.8849E-02	+1.2997E+00
6	+3.0480E+01	+5.9224E+01	+5.8998E+01	+3.8099E-01	+9.2071E-01
7	+3.9624E+01	+7.3552E+01	+7.2290E+01	+1.7163E+00	+5.9693E-01
8	+4.8768E+01	+8.7881E+01	+8.4761E+01	+3.5493E+00	+4.1815E-01
9	+6.0960E+01	+9.9343E+01	+9.9946E+01	-6.0689E-01	+3.2722E-01
10	+7.6200E+01	+1.1081E+02	+1.1667E+02	-5.2951E+00	+2.6302E-01
11	+9.1440E+01	+1.2800E+02	+1.3111E+02	-2.4315E+00	+1.9711E-01
12	+1.2192E+02	+1.5600E+02	+1.5400E+02	+1.2798E+00	+1.3270E-01
13	+1.5240E+02	+1.7200E+02	+1.7010E+02	+1.1057E+00	+1.0916E-01
14	+1.9812E+02	+1.8800E+02	+1.8400E+02	+2.1265E+00	+9.1370E-02
15	+2.4384E+02	+2.2100E+02	+1.8847E+02	+1.4717E+01	+6.6120E-04
16	+3.0480E+02	+2.0500E+02	+1.8438E+02	+1.0057E+01	+7.6844E-04
17	+3.9624E+02	+1.6500E+02	+1.6640E+02	-8.4802E-01	+1.1862E-01

## CORRELATION MATRIX:

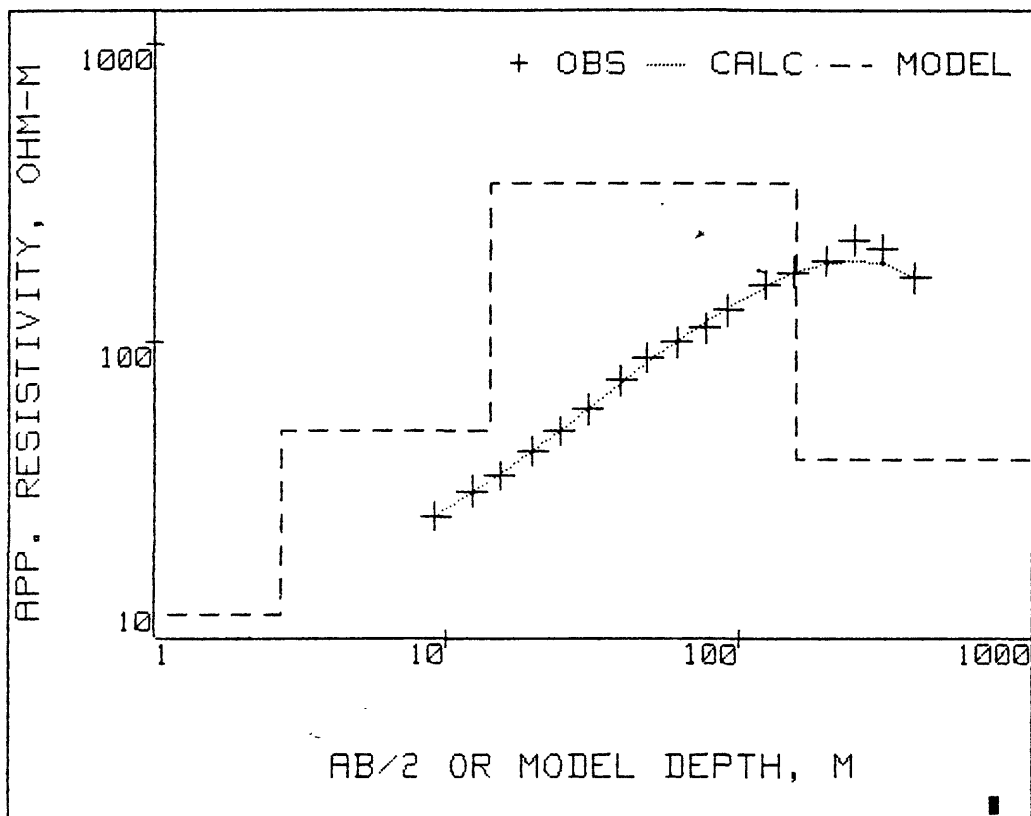
	2	3	5	6	7
2	+1.00	+.59	+.98	+.91	-.57
3	+.59	+1.00	+.51	+.81	-.97
5	+.98	+.51	+1.00	+.83	-.50
6	+.91	+.81	+.83	+1.00	-.77
7	-.57	-.97	-.50	-.77	+1.00

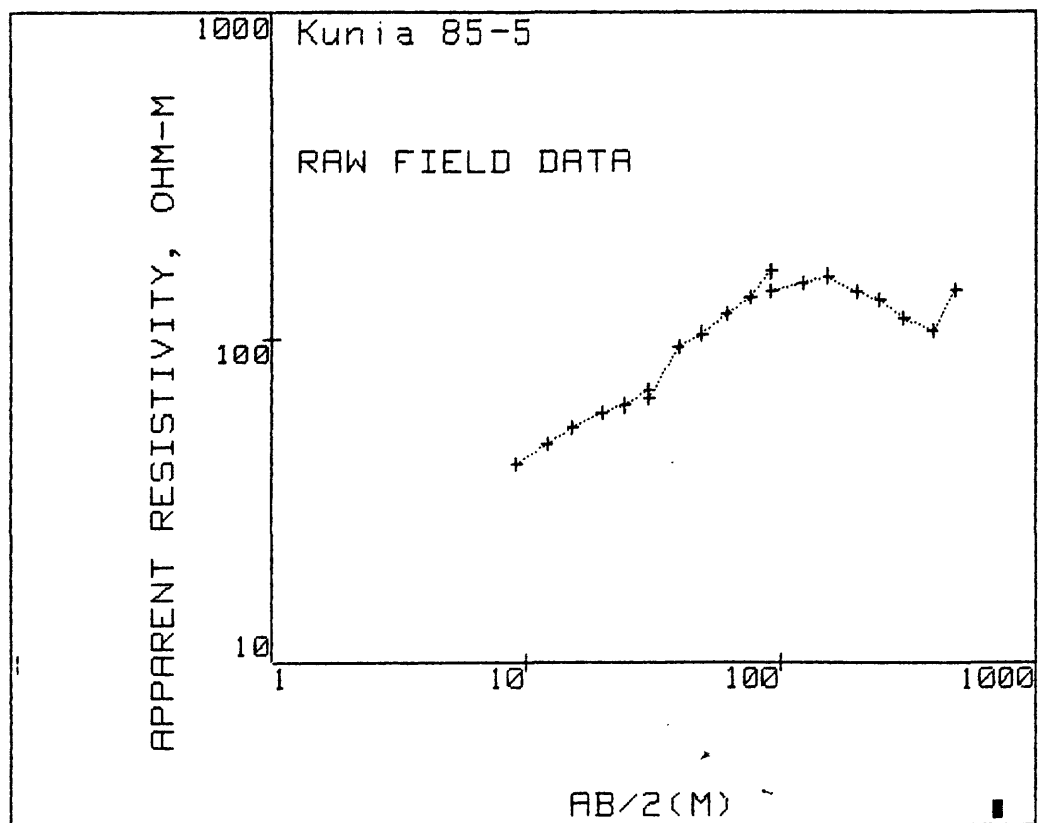
REDUCED CHI-SQUARED=5.812  
 PHI=63.932

DCLAG: \*\*\*\*\* END \*\*\*\*\* Kunia 85-4  
 COORDINATES: 0 0  
 ELEVATION : 123 METER  
 AZIMUTH :

RESISTIVITY			THICKNESS			DEPTH	ELEV
*****	12.0	*****	2.0	2.7	3.7	0.0	123.0
30.1	49.6	81.6	8.1	11.5	16.4	2.7	120.3
281.5	341.3	413.8	110.0	142.1	183.7	14.2	108.8
*****	40.0	*****				156.3	-33.3

Kunia 85-4





AB/2 (M) APP. RHO

9.1	41.3
12.2	47.5
15.2	53.5
19.8	59.1
24.4	62.3
30.5	69.2
30.5	65.5
39.6	94.0
48.8	103.0
61.0	118.0
76.2	133.0
91.4	159.0
91.4	139.0
121.9	147.0
152.4	154.0
198.1	139.0
243.8	131.0
304.8	115.0
396.2	105.0
487.7	141.0

## MARQUARDT STATISTICS: Kunia 85-5

	X	OBSERVED	PREDICTED	%RESIDUALS	WEIGHT FN
1	+9.1440E+00	+3.4175E+01	+3.4991E+01	-2.3884E+00	+4.0314E+00
2	+1.2192E+01	+3.9305E+01	+3.8586E+01	+1.8290E+00	+3.0477E+00
3	+1.5240E+01	+4.4270E+01	+4.2128E+01	+4.8375E+00	+2.4024E+00
4	+1.9812E+01	+4.8904E+01	+4.7883E+01	+2.0864E+00	+1.9687E+00
5	+2.4384E+01	+5.1551E+01	+5.4190E+01	-5.1192E+00	+1.7717E+00
6	+3.0480E+01	+5.7261E+01	+6.3040E+01	-1.0092E+01	+1.4360E+00
7	+3.9624E+01	+8.2176E+01	+7.6172E+01	+7.3059E+00	+6.9723E-03
8	+4.8768E+01	+9.0044E+01	+8.8288E+01	+1.9497E+00	+5.8071E-01
9	+6.0960E+01	+1.0316E+02	+1.0236E+02	+7.6874E-01	+4.4245E-01
10	+7.6200E+01	+1.1627E+02	+1.1662E+02	-3.0235E-01	+3.4828E-01
11	+9.1440E+01	+1.3900E+02	+1.2751E+02	+8.2683E+00	+2.4369E-01
12	+1.2192E+02	+1.4700E+02	+1.4088E+02	+4.1610E+00	+2.1789E-01
13	+1.5240E+02	+1.5400E+02	+1.4582E+02	+5.3133E+00	+1.9853E-01
14	+1.9812E+02	+1.3900E+02	+1.4336E+02	-3.1334E+00	+2.4369E-01
15	+2.4384E+02	+1.3100E+02	+1.3481E+02	-2.9097E+00	+2.7436E-01
16	+3.0480E+02	+1.1500E+02	+1.2057E+02	-4.8409E+00	+3.5602E-01
17	+3.9624E+02	+1.0500E+02	+1.0106E+02	+3.7479E+00	+4.2706E-01
18	+4.8768E+02	+1.4100E+02	+8.6944E+01	+3.8337E+01	+2.3683E-03

## CORRELATION MATRIX:

	2	4	5	6	7
2	+1.00	-.28	+.96	+.77	+.27
4	-.28	+1.00	-.24	-.45	-.96
5	+.96	-.24	+1.00	+.60	+.22
6	+.77	-.45	+.60	+1.00	+.46
7	+.27	-.96	+.22	+.46	+1.00

REDUCED CHI-SQUARED=29.52

PHI=354.24

DCLAG: \*\*\*\*\* END \*\*\*\*\*

Kunia 85-5

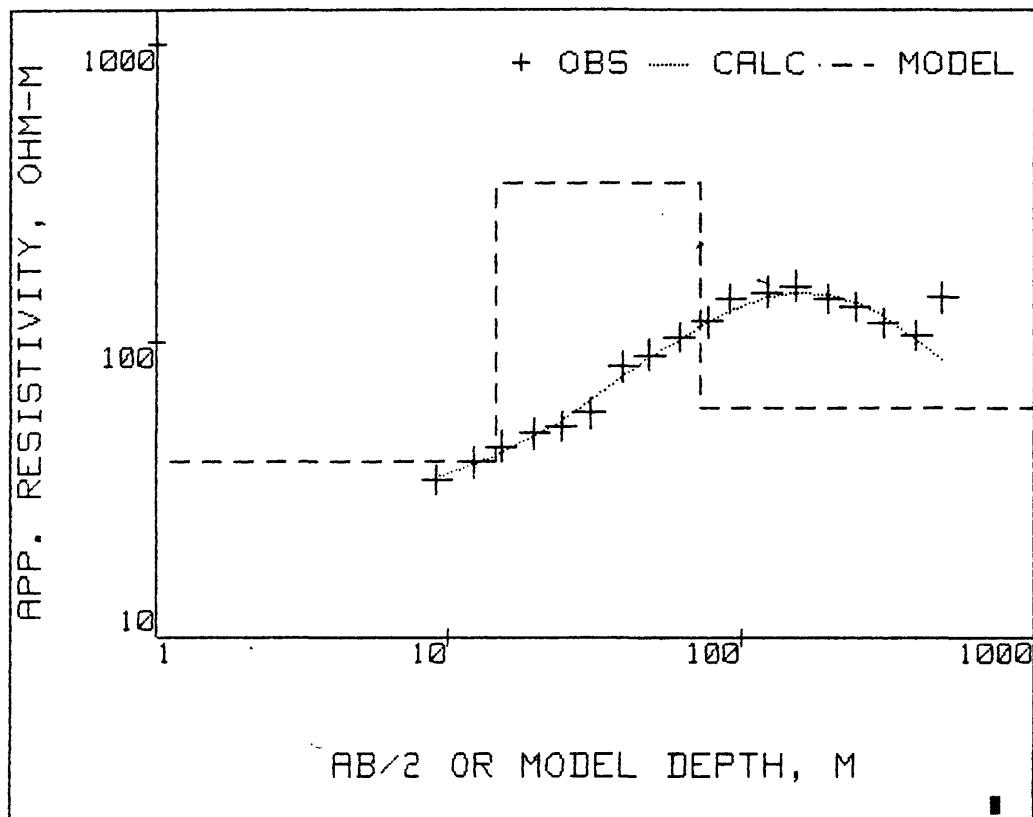
COORDINATES: 0 0

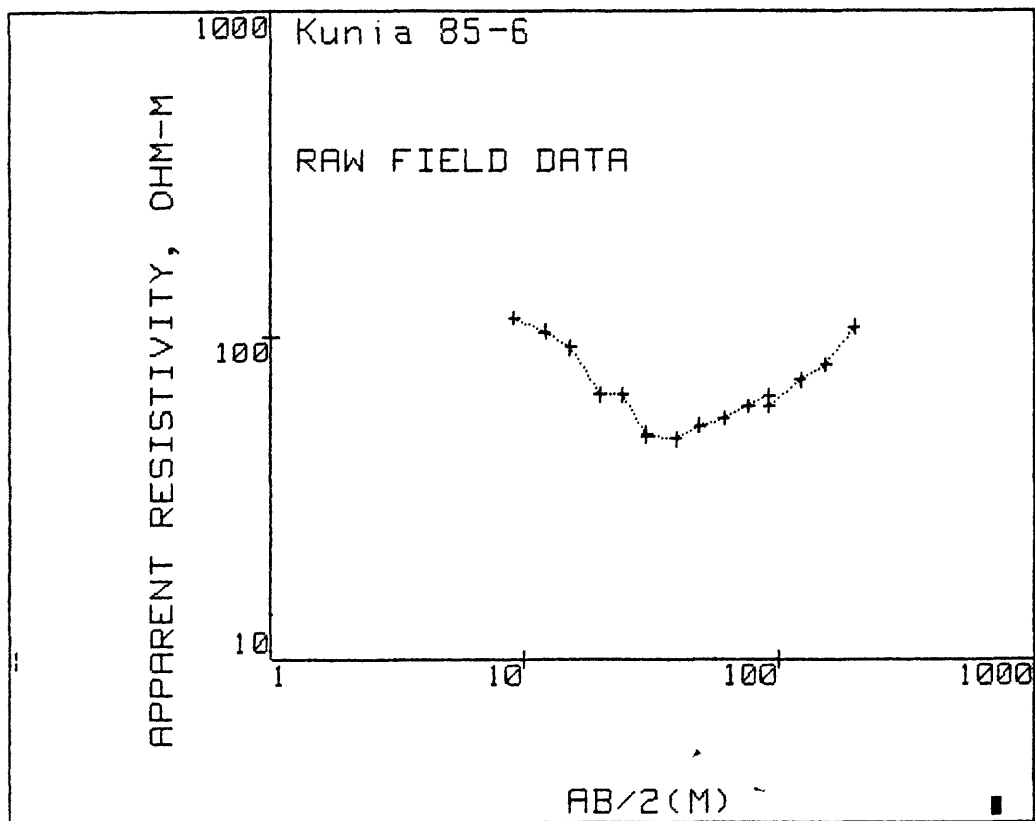
ELEVATION : 122 METER

AZIMUTH :

RESISTIVITY			THICKNESS			DEPTH	ELEV
*****	12.0*****		.3	.9	2.7	0.0	122.0
29.2	39.6	53.7	11.6	13.6	16.0	.9	121.1
*****	340.0*****		45.1	57.6	73.5	14.5	107.5
40.9	59.0	85.2				72.1	49.9

Kunia 85-5





AB/2 (M) APP. RHO

9.1	113.0
12.2	103.0
15.2	92.0
19.8	66.0
24.4	66.0
30.5	50.0
30.5	49.0
39.6	48.0
48.8	53.0
61.0	56.0
76.2	61.0
91.4	65.0
91.4	61.0
121.9	73.0
152.4	81.0
198.1	106.0

## MARQUARDT STATISTICS: Kunia 85-6

	X	OBSERVED	PREDICTED	%RESIDUALS	WEIGHT FN
1	+9.1440E+00	+1.0393E+02	+1.0805E+02	-3.9703E+00	+3.5793E-01
2	+1.2192E+01	+9.4728E+01	+9.2425E+01	+2.4313E+00	+4.3080E-01
3	+1.5240E+01	+8.4612E+01	+7.8879E+01	+6.7751E+00	+5.3998E-01
4	+1.9812E+01	+6.0700E+01	+6.4400E+01	-6.0967E+00	+1.0492E+00
5	+2.4384E+01	+6.0700E+01	+5.5817E+01	+8.0436E+00	+1.0492E+00
6	+3.0480E+01	+4.5985E+01	+5.0036E+01	-8.8107E+00	+1.8282E+00
7	+3.9624E+01	+4.5046E+01	+4.7246E+01	-4.8845E+00	+1.9051E+00
8	+4.8768E+01	+4.9738E+01	+4.7457E+01	+4.5873E+00	+1.5626E+00
9	+6.0960E+01	+5.2554E+01	+4.9790E+01	+5.2594E+00	+1.3997E+00
10	+7.6200E+01	+5.7246E+01	+5.4469E+01	+4.8513E+00	+1.1796E+00
11	+9.1440E+01	+6.1000E+01	+6.0259E+01	+1.2142E+00	+1.0389E+00
12	+1.2192E+02	+7.3000E+01	+7.3241E+01	-3.2962E-01	+7.2543E-01
13	+1.5240E+02	+8.1000E+01	+8.6404E+01	-6.6715E+00	+5.8921E-01
14	+1.9812E+02	+1.0600E+02	+1.0489E+02	+1.0477E+00	+3.4406E-01

## CORRELATION MATRIX:

	1	2	4	5
1	+1.00	+.55	-.87	+.52
2	+.55	+1.00	-.79	+.92
4	-.87	-.79	+1.00	-.73
5	+.52	+.92	-.73	+1.00

REDUCED CHI-SQUARED=43.37  
PHI=390.36

DCLAG: \*\*\*\*\* END \*\*\*\*\* Kunia 85-6

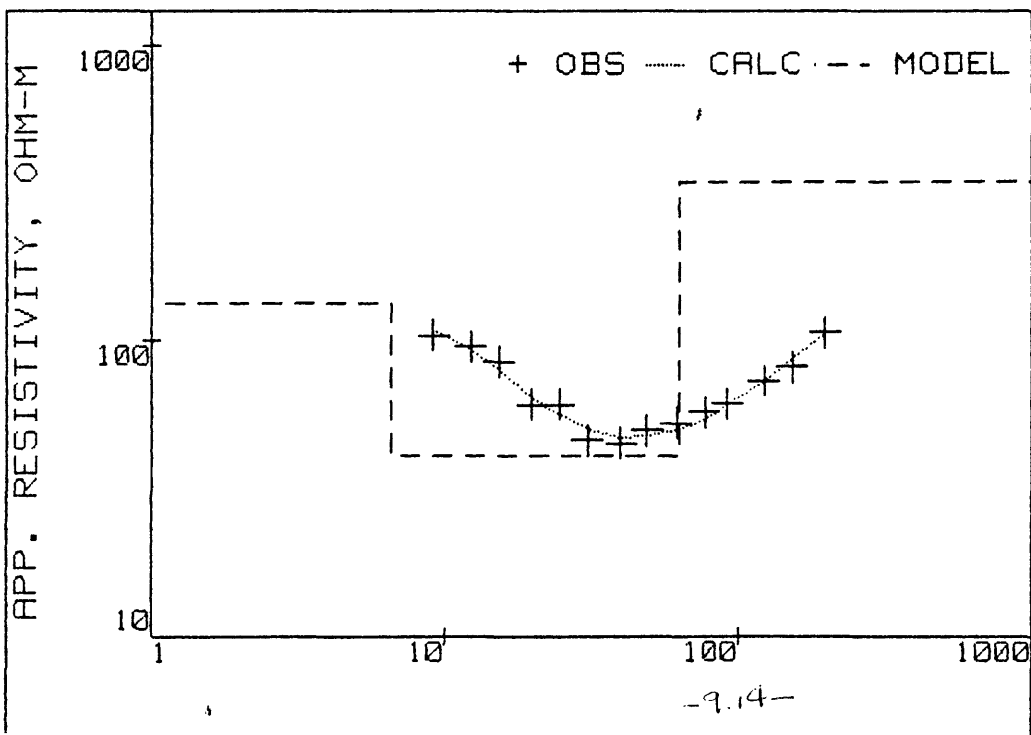
COORDINATES: 0 0

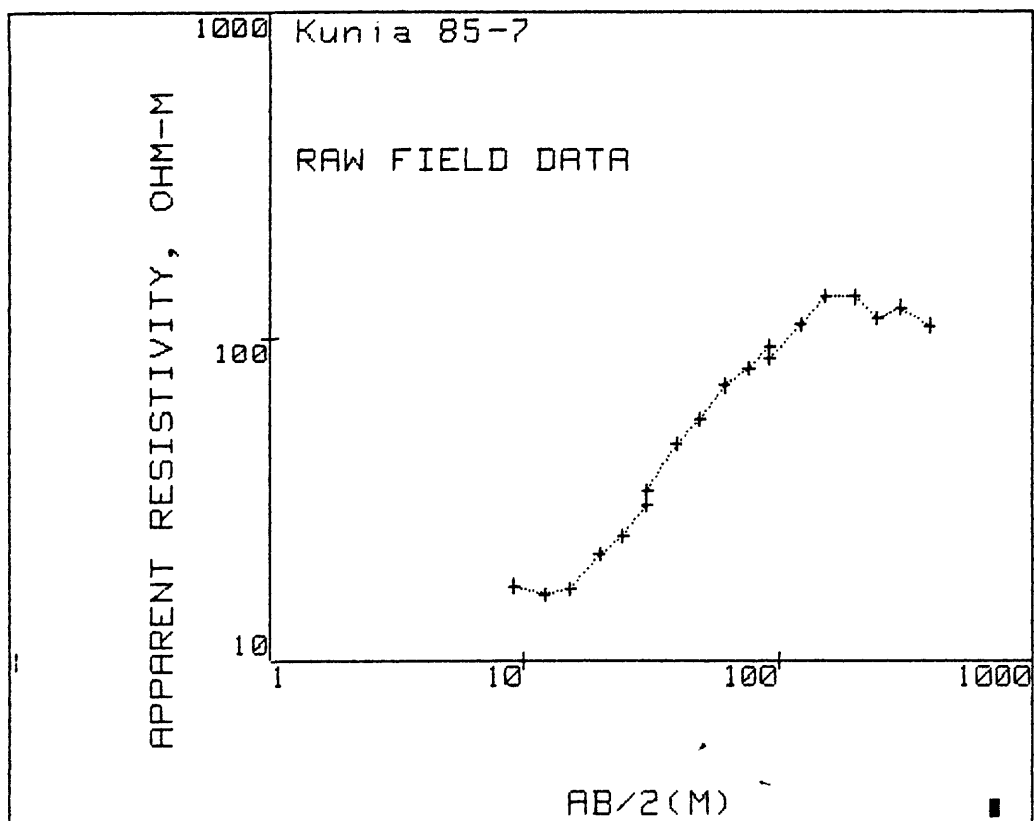
ELEVATION : 98 METER

AZIMUTH :

RESISTIVITY			THICKNESS			DEPTH	ELEV
111.2	132.4	157.6	5.3	6.5	8.0	0.0	98.0
36.5	40.7	45.4	46.5	55.3	65.8	6.5	91.5
*****	340.0*****					61.8	36.2

Kunia 85-6





AB/2(M) APP.RHO

9.1	17.2
12.2	16.1
15.2	16.9
19.8	21.6
24.4	24.5
30.5	30.5
30.5	33.6
39.6	47.0
48.8	56.0
61.0	71.0
76.2	80.0
91.4	94.0
91.4	86.0
121.9	110.0
152.4	135.0
198.1	134.0
243.8	115.0
304.8	124.0
396.2	109.0



## MARQUARDT STATISTICS: Kunia 85-7

	X	OBSERVED	PREDICTED	%RESIDUALS	WEIGHT FN
1	+9.1440E+00	+1.7336E+01	+1.6999E+01	+1.9391E+00	+3.2881E+00
2	+1.2192E+01	+1.6227E+01	+1.6791E+01	-3.4760E+00	+3.7527E+00
3	+1.5240E+01	+1.7033E+01	+1.8797E+01	-1.0353E+01	+3.4058E+00
4	+1.9812E+01	+2.1770E+01	+2.2859E+01	-5.0008E+00	+2.0849E+00
5	+2.4384E+01	+2.4693E+01	+2.7306E+01	-1.0581E+01	+1.6206E+00
6	+3.0480E+01	+3.0740E+01	+3.3294E+01	-8.3059E+00	+1.0457E+00
7	+3.9624E+01	+4.3000E+01	+4.1958E+01	+2.4241E+00	+5.3442E-01
8	+4.8768E+01	+5.1234E+01	+5.0130E+01	+2.1544E+00	+3.7644E-01
9	+6.0960E+01	+6.4957E+01	+6.0245E+01	+7.2554E+00	+2.3419E-01
10	+7.6200E+01	+7.3191E+01	+7.1676E+01	+2.0699E+00	+1.8446E-01
11	+9.1440E+01	+8.6000E+01	+8.1813E+01	+4.8681E+00	+1.3360E-01
12	+1.2192E+02	+1.1000E+02	+9.8458E+01	+1.0493E+01	+8.1664E-02
13	+1.5240E+02	+1.3500E+02	+1.1070E+02	+1.7998E+01	+5.4219E-02
14	+1.9812E+02	+1.3400E+02	+1.2215E+02	+8.8403E+00	+5.5031E-02
15	+2.4384E+02	+1.1500E+02	+1.2714E+02	-1.0556E+01	+7.4717E-04
16	+3.0480E+02	+1.2400E+02	+1.2684E+02	-2.2864E+00	+6.4265E-02
17	+3.9624E+02	+1.0900E+02	+1.1803E+02	-8.2837E+00	+8.3170E-02

## CORRELATION MATRIX:

	1	5	6	7
1	+1.00	-.99	+.89	-.09
5	-.99	+1.00	-.87	+.10
6	+.89	-.87	+1.00	+.05
7	-.09	+.10	+.05	+1.00

REDUCED CHI-SQUARED=83.94

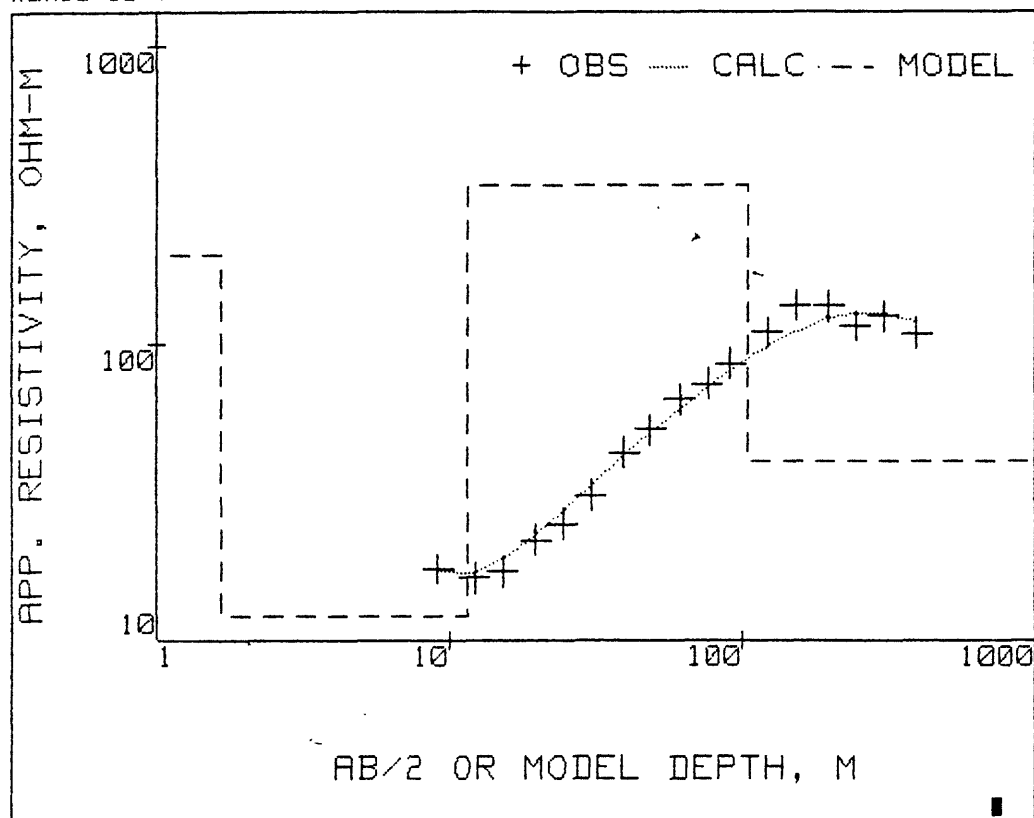
PHI=1007.3

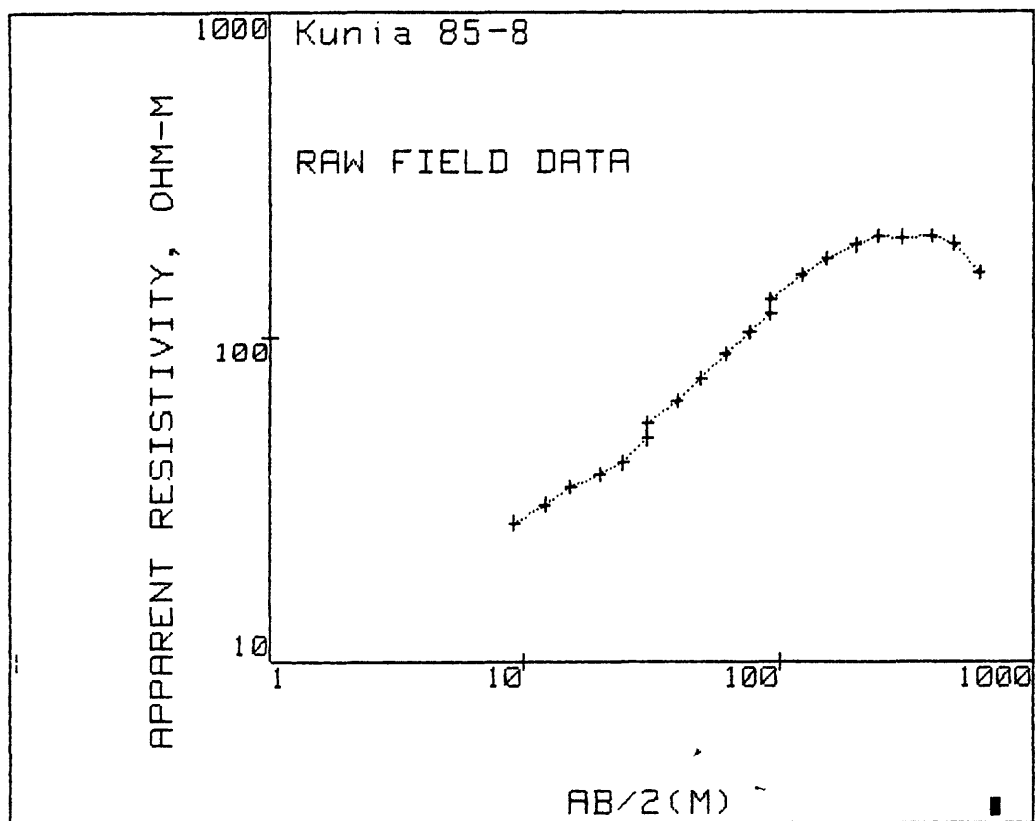
DCLAG: \*\*\*\*\* END \*\*\*\*\*  
 COORDINATES: 0 0  
 ELEVATION : 110 METER  
 AZIMUTH :

Kunia 85-7

RESISTIVITY		THICKNESS			DEPTH	ELEV
0.0	200.0	.1	1.7	19.4	0.0	110.0
*****	12.0*****	7.8	9.9	12.6	1.7	108.3
*****	340.0*****	64.4	92.7	133.6	11.6	98.4
*****	40.0*****				104.3	5.7

Kunia 85-7





AB/2 (M) APP. RHO

9.1	26.9
12.2	30.6
15.2	34.7
19.8	37.9
24.4	41.0
30.5	48.8
30.5	54.2
39.6	63.3
48.8	74.5
61.0	88.2
76.2	104.0
91.4	119.0
91.4	130.0
121.9	156.0
152.4	174.0
198.1	192.0
243.8	204.0
304.8	203.0
396.2	204.0
487.7	194.0
609.6	158.0

## MARQUARDT STATISTICS: Kunia 85-8

	X	OBSERVED	PREDICTED	%RESIDUALS	WEIGHT FN
1	+9.1440E+00	+3.2638E+01	+3.2902E+01	-8.0904E-01	+4.2114E+00
2	+1.2192E+01	+3.7128E+01	+3.7222E+01	-2.5421E-01	+3.2545E+00
3	+1.5240E+01	+4.2102E+01	+4.0852E+01	+2.9686E+00	+2.5309E+00
4	+1.9812E+01	+4.5985E+01	+4.5984E+01	+1.9161E-03	+2.1215E+00
5	+2.4384E+01	+4.9746E+01	+5.1201E+01	-2.9244E+00	+1.8128E+00
6	+3.0480E+01	+5.9210E+01	+5.8514E+01	+1.1751E+00	+1.2796E+00
7	+3.9624E+01	+6.9151E+01	+7.0073E+01	-1.3329E+00	+9.3816E-01
8	+4.8768E+01	+8.1387E+01	+8.1639E+01	-3.1075E-01	+6.7729E-01
9	+6.0960E+01	+9.6353E+01	+9.6403E+01	-5.1565E-02	+4.8322E-01
10	+7.6200E+01	+1.1361E+02	+1.1323E+02	+3.3606E-01	+3.4755E-01
11	+9.1440E+01	+1.3000E+02	+1.2824E+02	+1.3561E+00	+2.6546E-01
12	+1.2192E+02	+1.5600E+02	+1.5332E+02	+1.7155E+00	+1.8434E-01
13	+1.5240E+02	+1.7400E+02	+1.7276E+02	+7.1547E-01	+1.4818E-01
14	+1.9812E+02	+1.9200E+02	+1.9302E+02	-5.2907E-01	+1.2170E-01
15	+2.4384E+02	+2.0400E+02	+2.0473E+02	-3.5638E-01	+1.0780E-01
16	+3.0480E+02	+2.0300E+02	+2.1012E+02	-3.5093E+00	+1.0886E-01
17	+3.9624E+02	+2.0400E+02	+2.0357E+02	+2.1126E-01	+1.0780E-01
18	+4.8768E+02	+1.9400E+02	+1.8731E+02	+3.4507E+00	+1.1920E-01
19	+6.0960E+02	+1.5800E+02	+1.6012E+02	-1.3411E+00	+1.7971E-01

## CORRELATION MATRIX:

	1	2	3	4	5	6	7
1	+1.00	+.06	-.20	-.51	+1.00	-.50	+.38
2	+.06	+1.00	+.50	+.21	+.09	+.71	-.35
3	-.20	+.50	+1.00	+.74	-.19	+.80	-.91
4	-.51	+.21	+.74	+1.00	-.51	+.63	-.95
5	+1.00	+.09	-.19	-.51	+1.00	-.48	+.37
6	-.50	+.71	+.80	+.63	-.48	+1.00	-.73
7	+.38	-.35	-.91	-.95	+.37	-.73	+1.00

REDUCED CHI-SQUARED=4.838

PHI=53.22

DCLAG: \*\*\*\*\* END \*\*\*\*\*

Kunia 85-8

COORDINATES: 0 0

ELEVATION : 104 METER

AZIMUTH :

B-SD	B	B+SD
.001	5.965	36983.715
41.105	46.208	51.945
310.289	362.334	423.108
11.199	43.568	169.495
0.000	.690	5288.068
15.214	17.429	19.965
120.519	189.592	298.254

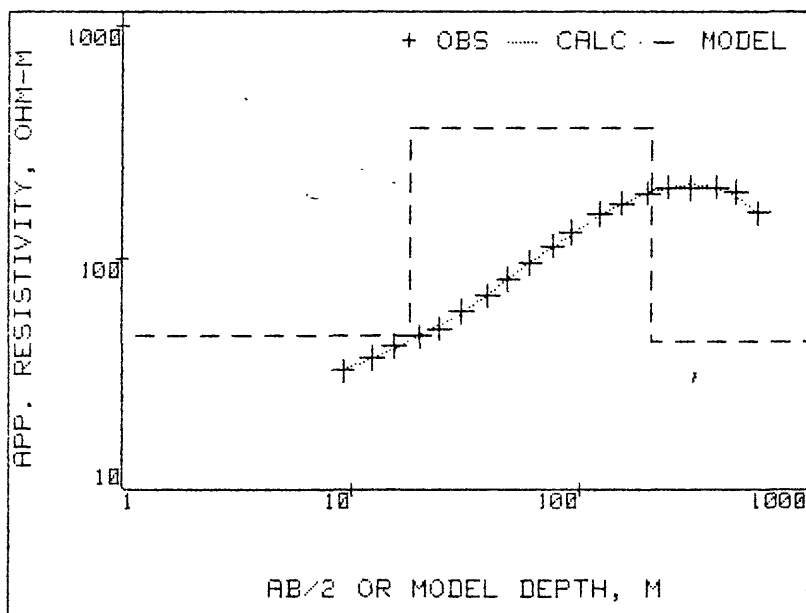
FINAL UNSCALED PARAMETERS--  
(\* denotes fixed value)

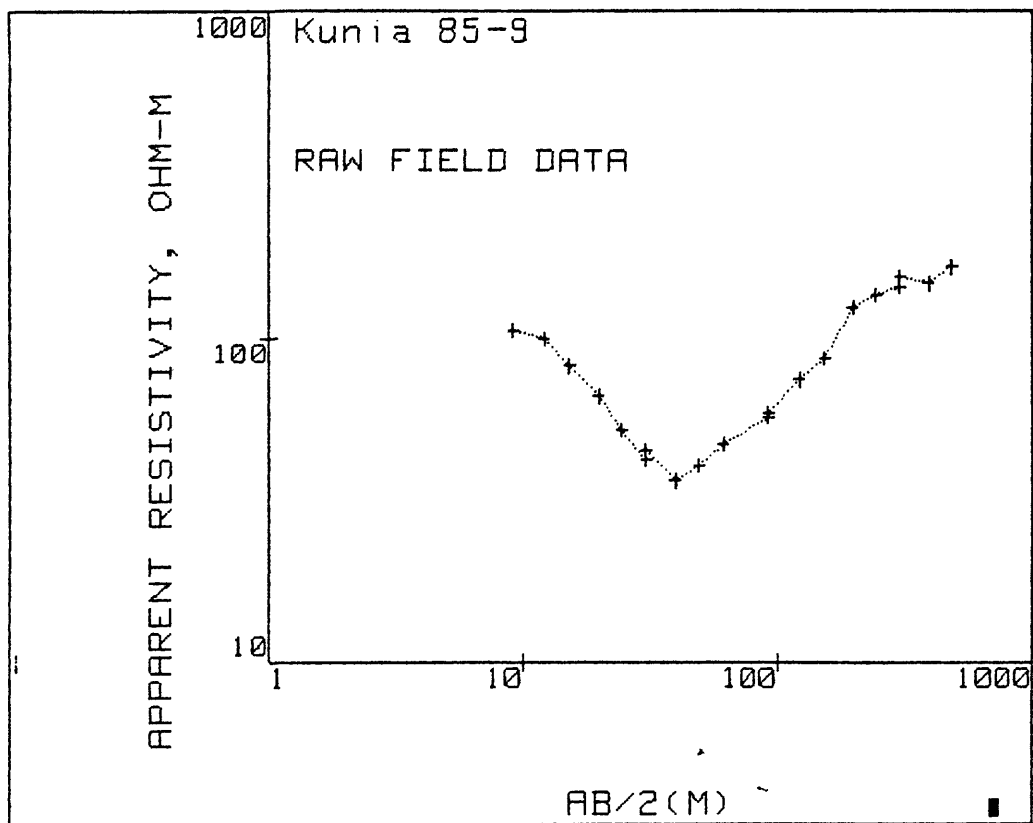
RESISTIVITY

DEPTH

1	5.965	1	5.965
2	46.208	2	* 46.208
3	362.334	3	362.334
4	43.568	4	43.568
5	.690	1	.690
6	17.429	2	18.119
7	189.592	3	207.711

Kunia 85-8





AB/2(M) APP.RHO

9.1	105.0
12.2	99.0
15.2	82.0
19.8	66.0
24.4	52.0
30.5	42.0
30.5	45.0
39.6	36.0
48.8	40.0
61.0	47.0
91.4	57.0
91.4	58.0
121.9	74.0
152.4	86.0
198.1	123.0
243.8	135.0
304.8	142.0
304.8	153.0
396.2	146.0
487.7	164.0

## MARQUARDT STATISTICS: Kunia 85-9

	X	OBSERVED	PREDICTED	%RESIDUALS	WEIGHT FN
1	+9.1440E+00	+1.2334E+02	+1.2487E+02	-1.2358E+00	+3.2944E-01
2	+1.2192E+01	+1.1629E+02	+1.1239E+02	+3.3589E+00	+3.7058E-01
3	+1.5240E+01	+9.6324E+01	+9.8144E+01	-1.8898E+00	+5.4017E-01
4	+1.9812E+01	+7.7529E+01	+7.7682E+01	-1.9802E-01	+8.3381E-01
5	+2.4384E+01	+6.1083E+01	+6.1563E+01	-7.8486E-01	+1.3432E+00
6	+3.0480E+01	+4.9337E+01	+4.8136E+01	+2.4336E+00	+2.0590E+00
7	+3.9624E+01	+3.9469E+01	+4.1045E+01	-3.9919E+00	+3.2172E+00
8	+4.8768E+01	+4.3855E+01	+4.2261E+01	+3.6337E+00	+2.6059E+00
9	+6.0960E+01	+5.1529E+01	+4.8508E+01	+5.8641E+00	+1.8875E+00
10	+9.1440E+01	+6.2493E+01	+6.7200E+01	-7.5326E+00	+1.2833E+00
11	+1.2192E+02	+7.9732E+01	+8.4134E+01	-5.5203E+00	+7.8836E-01
12	+1.5240E+02	+9.2662E+01	+9.8917E+01	-6.7506E+00	+5.8370E-01
13	+1.9812E+02	+1.3253E+02	+1.1744E+02	+1.1384E+01	+2.8535E-01
14	+2.4384E+02	+1.4546E+02	+1.3205E+02	+9.2159E+00	+2.3688E-01
15	+3.0480E+02	+1.5300E+02	+1.4623E+02	+4.4237E+00	+2.1410E-01
16	+3.9624E+02	+1.4600E+02	+1.5817E+02	-8.3365E+00	+2.3512E-01
17	+4.8768E+02	+1.6400E+02	+1.6163E+02	+1.4470E+00	+1.8634E-01

## CORRELATION MATRIX:

	1	4	5	6	7
1	+1.00	+1.12	-.80	-.10	-.13
4	+1.12	+1.00	-.22	-.54	-1.00
5	-.80	-.22	+1.00	+.29	+.23
6	-.10	-.54	+.29	+1.00	+.58
7	-.13	-1.00	+.23	+.58	+1.00

REDUCED CHI-SQUARED=47.72

PHI=524.96

DCLAG: \*\*\*\*\* END \*\*\*\*\*

Kunia 85-9

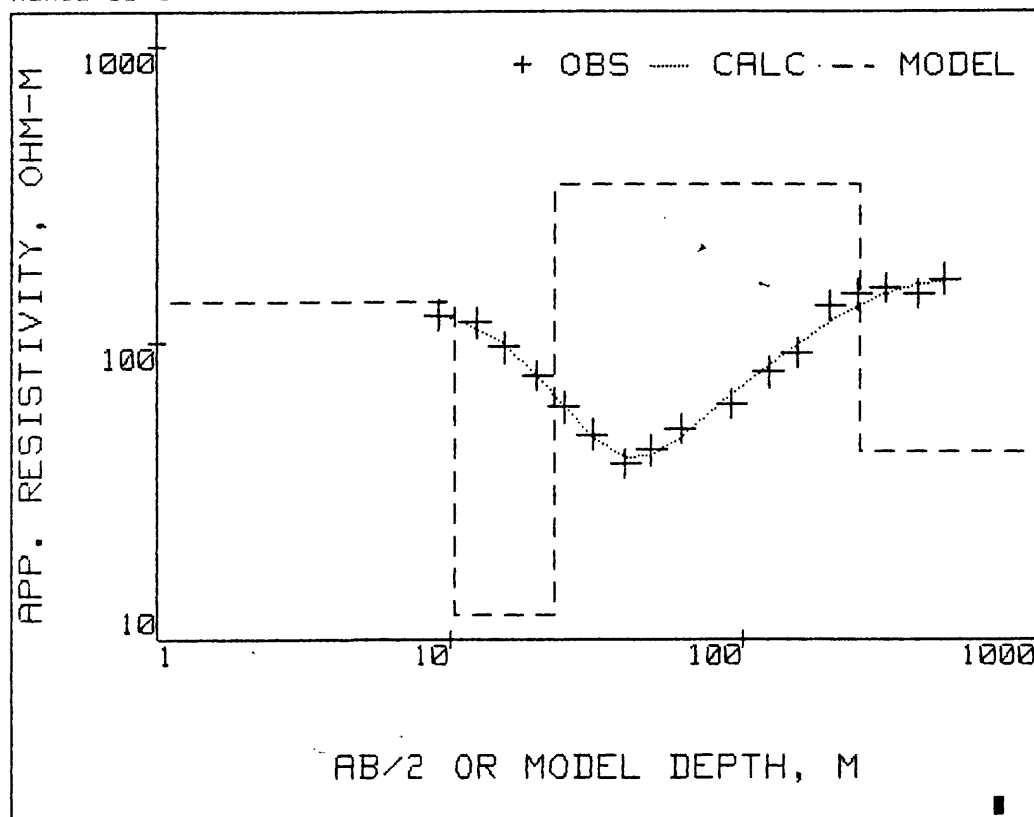
COORDINATES: 0 0

ELEVATION : 195 METER

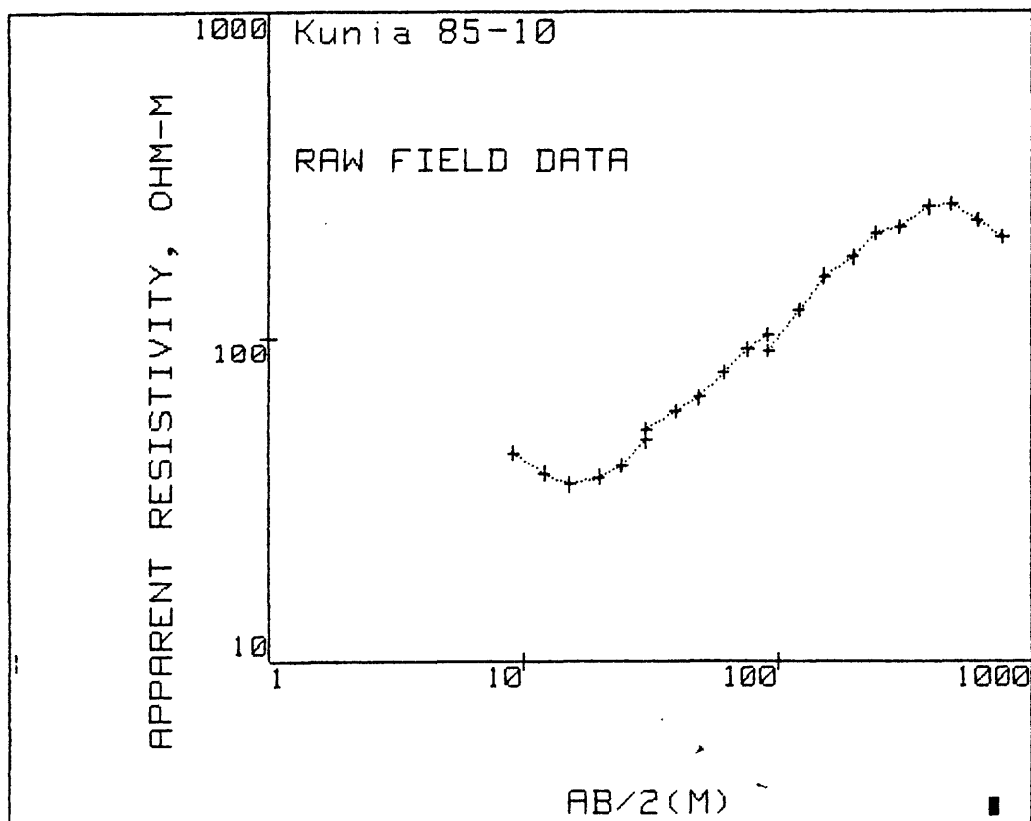
AZIMUTH :

RESISTIVITY			THICKNESS			DEPTH	ELEV
127.4	138.1	149.8	9.7	10.3	11.1	0.0	195.0
*****	12.0*****		11.7	12.5	13.3	10.3	184.7
*****	340.0*****		18.1	226.4	2835.9	22.8	172.2
0.0	43.1					249.2	-54.2

Kunia 85-9







AB/2(M) APP.RHO

9.1	44.0
12.2	38.0
15.2	35.0
19.8	37.0
24.4	40.0
30.5	48.0
30.5	52.0
39.6	59.0
48.8	65.0
61.0	78.0
76.2	92.0
91.4	102.0
91.4	91.0
121.9	122.0
152.4	154.0
198.1	176.0
243.8	207.0
304.8	216.0
396.2	249.0
487.7	255.0
609.6	226.0
762.0	201.0

## MARQUARDT STATISTICS: Kunia 85-10

	X	OBSERVED	PREDICTED	%RESIDUALS	WEIGHT FN
1	+9.1440E+00	+4.2526E+01	+4.2678E+01	-3.5599E-01	+2.0180E+00
2	+1.2192E+01	+3.6727E+01	+3.6156E+01	+1.5554E+00	+2.7056E+00
3	+1.5240E+01	+3.3828E+01	+3.4487E+01	-1.9478E+00	+3.1893E+00
4	+1.9812E+01	+3.5761E+01	+3.5786E+01	-7.2198E-02	+2.8538E+00
5	+2.4384E+01	+3.8660E+01	+3.8794E+01	-3.4569E-01	+2.4418E+00
6	+3.0480E+01	+4.6392E+01	+4.3857E+01	+5.4639E+00	+1.6957E+00
7	+3.9624E+01	+5.2637E+01	+5.2488E+01	+2.8444E-01	+1.3172E+00
8	+4.8768E+01	+5.7990E+01	+6.1520E+01	-6.0876E+00	+1.0853E+00
9	+6.0960E+01	+6.9588E+01	+7.3368E+01	-5.4321E+00	+7.5365E-01
10	+7.6200E+01	+8.2078E+01	+8.7312E+01	-6.3769E+00	+5.4173E-01
11	+9.1440E+01	+9.1000E+01	+1.0017E+02	-1.0075E+01	+4.4072E-01
12	+1.2192E+02	+1.2200E+02	+1.2289E+02	-7.3291E-01	+2.4520E-01
13	+1.5240E+02	+1.5400E+02	+1.4221E+02	+7.6554E+00	+1.5389E-01
14	+1.9812E+02	+1.7600E+02	+1.6599E+02	+5.6880E+00	+1.1782E-01
15	+2.4384E+02	+2.0700E+02	+1.8470E+02	+1.0771E+01	+8.5173E-02
16	+3.0480E+02	+2.1600E+02	+2.0335E+02	+5.8549E+00	+7.8223E-02
17	+3.9624E+02	+2.4900E+02	+2.2079E+02	+1.1329E+01	+5.8863E-02
18	+4.8768E+02	+2.5500E+02	+2.2861E+02	+1.0348E+01	+5.6126E-02
19	+6.0960E+02	+2.2600E+02	+2.2831E+02	-1.0224E+00	+7.1454E-02
20	+7.6200E+02	+2.0100E+02	+2.1669E+02	-7.8054E+00	+9.0334E-02

## CORRELATION MATRIX:

	1	3	6	7	8	9
1	+1.00	-.84	-.99	-.88	+.89	-.06
3	-.84	+1.00	+.90	+.99	-.62	+.11
6	-.99	+.90	+1.00	+.94	-.88	+.07
7	-.88	+.99	+.94	+1.00	-.72	+.09
8	+.89	-.62	-.88	-.72	+1.00	+.02
9	-.06	+.11	+.07	+.09	+.02	+1.00

REDUCED CHI-SQUARED=60.33

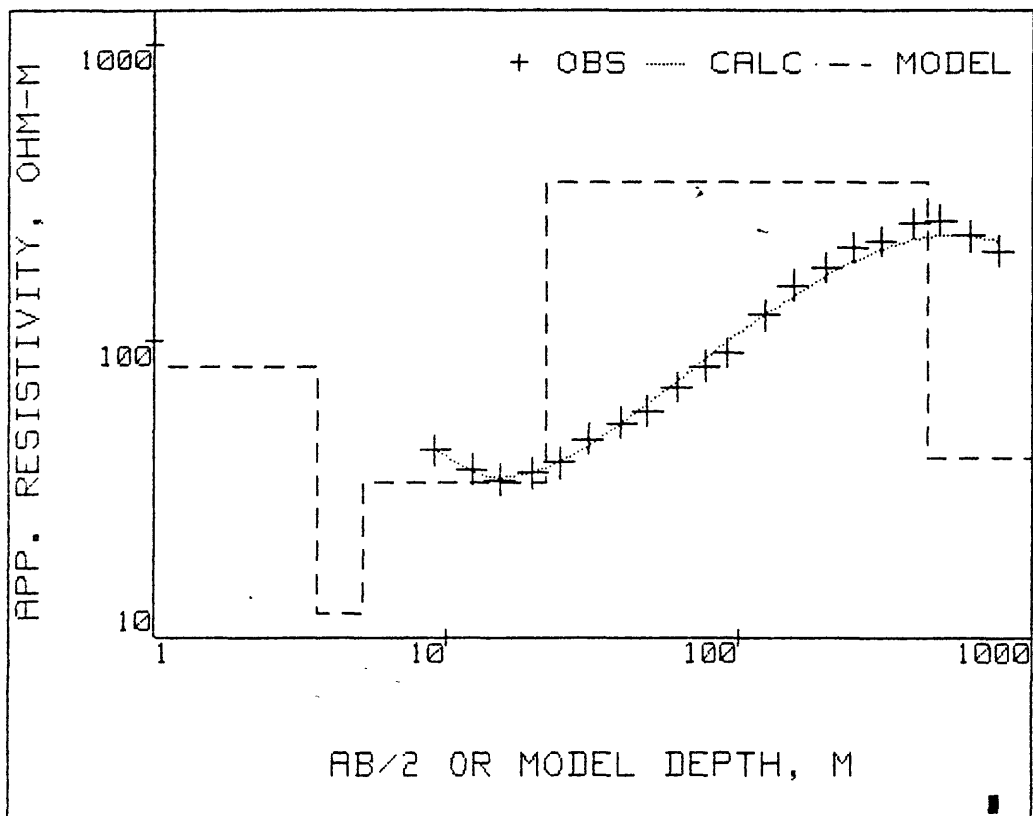
PHI=784.34

DCLAG: \*\*\*\*\* END \*\*\*\*\*  
 COORDINATES: 0 0  
 ELEVATION : 174 METER  
 AZIMUTH :

Kunia 85-10

RESISTIVITY			THICKNESS			DEPTH	ELEV
3.6	81.4	1865.2	.3	3.6	45.1	0.0	174.0
*****	12.0*****		0.0	1.6	1478.2	3.6	170.4
6.0	33.3	184.2	8.9	16.9	32.2	5.2	168.8
*****	340.0*****		343.2	418.1	509.4	22.1	151.9
*****	40.0*****					440.2	-266.2

Kunia 85-10



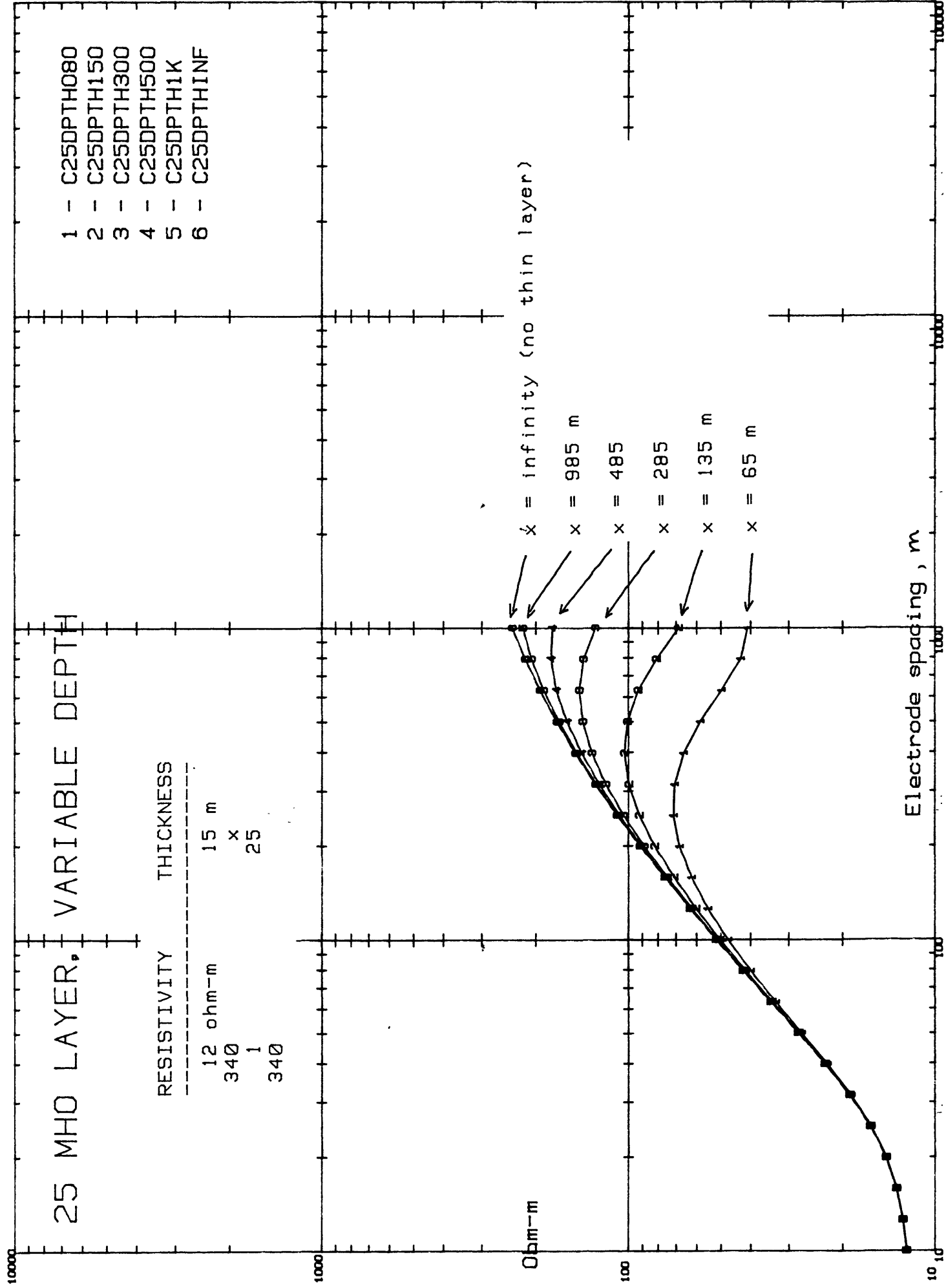
## List of Figures

- Figure 1. Six theoretical model curves computed for the following model:  $\rho_{01}=12$  ohm-m,  $\rho_{02}=\rho_{04}=340$  ohm-m,  $\rho_{03}=1$  ohm-m, thickness<sub>1</sub>=15 m, thickness<sub>3</sub>=25 m. The value of thickness<sub>2</sub> was given values (in meters) of 80, 150, 300, 500, 1000, and infinity. Each curve is identified in the upper right corner with a name composed of the conductance of the thin layer (C25) and the depth of its upper surface from the ground surface (DPTH080 for 80 m, for example). The curves representing models with a small depth to the thin, low-resistivity layer depart from the curve identified as C25DPTHINF at proportionately small electrode spacings.
- Figure 2. Four theoretical model curves computed for the following model:  $\rho_{01}=12$  ohm-m,  $\rho_{02}=\rho_{04}=340$  ohm-m, thickness<sub>1</sub>=15 m, thickness<sub>2</sub>=65 m, and thickness<sub>3</sub>=25 m. Parameter  $\rho_{03}$ , the resistivity of the thin layer, is given values of 1, 3, and 10 ohm-m. The fourth curve, labeled C25DPTHINF, has no thin, low-resistivity layer. Note that all three curves depart from this fourth curve at about the same electrode spacing.
- Figure 3. A map of the study area showing the town of Waipahu, Kunia Road and H-1 Freeway (thick solid lines), the nine useable Schlumberger soundings (thin solid lines), and the two profiles (thick dashed lines) shown in detail in Figures 5 and 6.
- Figure 4. Plot of the shifted field data for soundings 7, 1, 5, 4, and 8 with the electrode spacings normalized by the sounding elevation. Note that the apparent resistivities depart from a general, approximately 45° increasing trend at increasingly greater electrode spacings as one moves eastward. Compare this data plot with the model curves in Figure 1.
- Figure 5. Geoelectric profile along the 122 m (400 foot) elevation contour. Profile location is shown in Figure 1. Note the line marking the interface between the 340 and 40 ohm-m layers that dips eastward (to the right). Soundings 1 and 7 were made over Wai'anae lavas so that the subsurface conductor at sea level probably represents water table and not the clayey soil of the barrier layer.

Figure 6. Geoelectric profile along the 213 m (700 foot) elevation contour. Profile location is shown in Figure 1. Sounding 2 was made over Wai'anae lavas so that the subsurface conductor is probably related to groundwater stratification than to the clayey soil of the barrier layer.

Figure 7. A map of the study area showing the Schlumberger sounding locations (thin solid lines), major geologic contacts (thin dashed lines), the estimated location of the aquiclude at sea level (thick dashed line), and the location of the 1986 drilling.

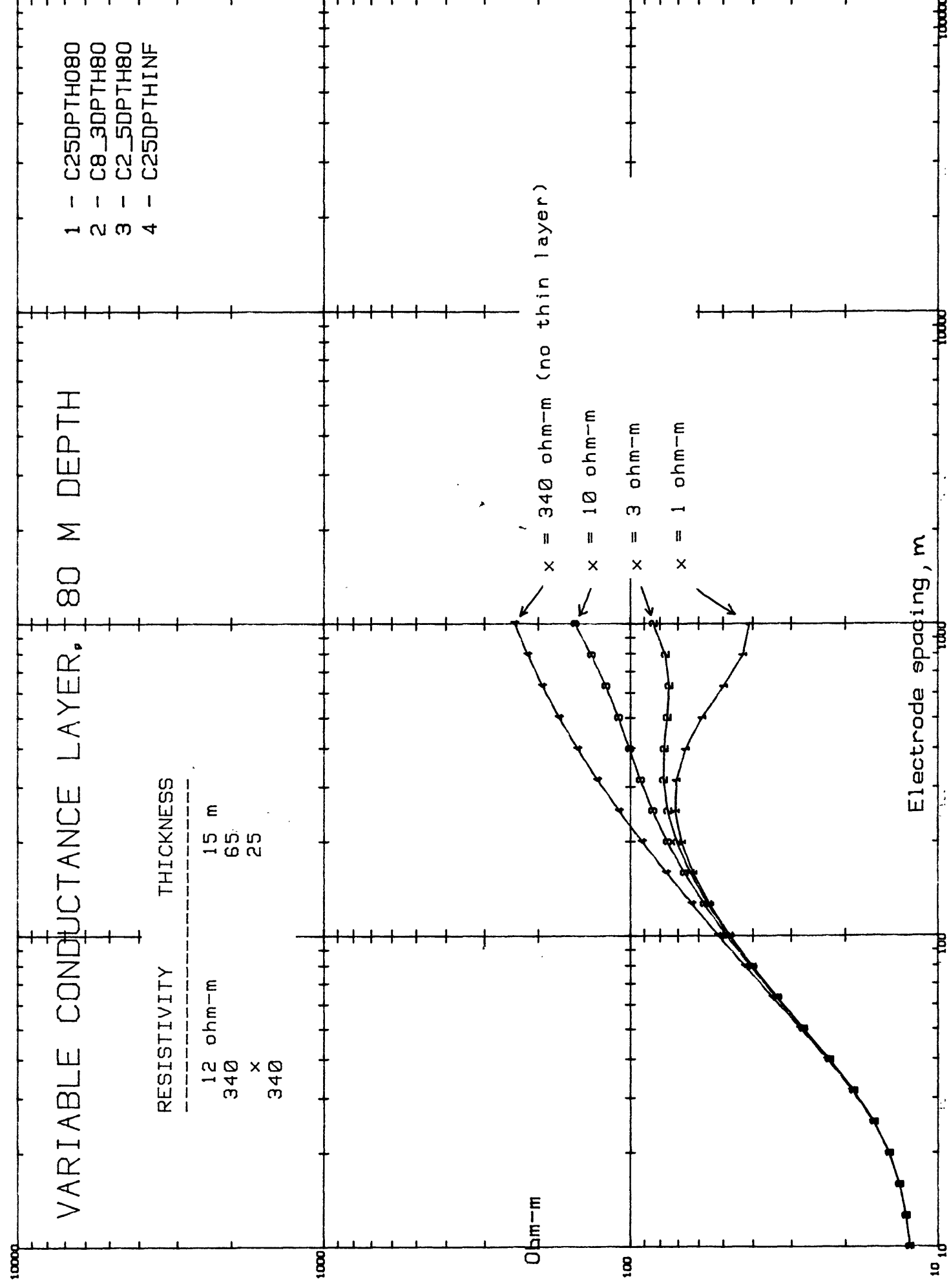
FIG. 1



# VARIABLE CONDUCTANCE LAYER, 80 M DEPTH

- 1 - C25DPTH080
- 2 - C8\_3DPTH80
- 3 - C2\_5DPTH80
- 4 - C25DPTHINF

RESISTIVITY	THICKNESS
12 ohm-m	15 m
340	65
x	25
340	



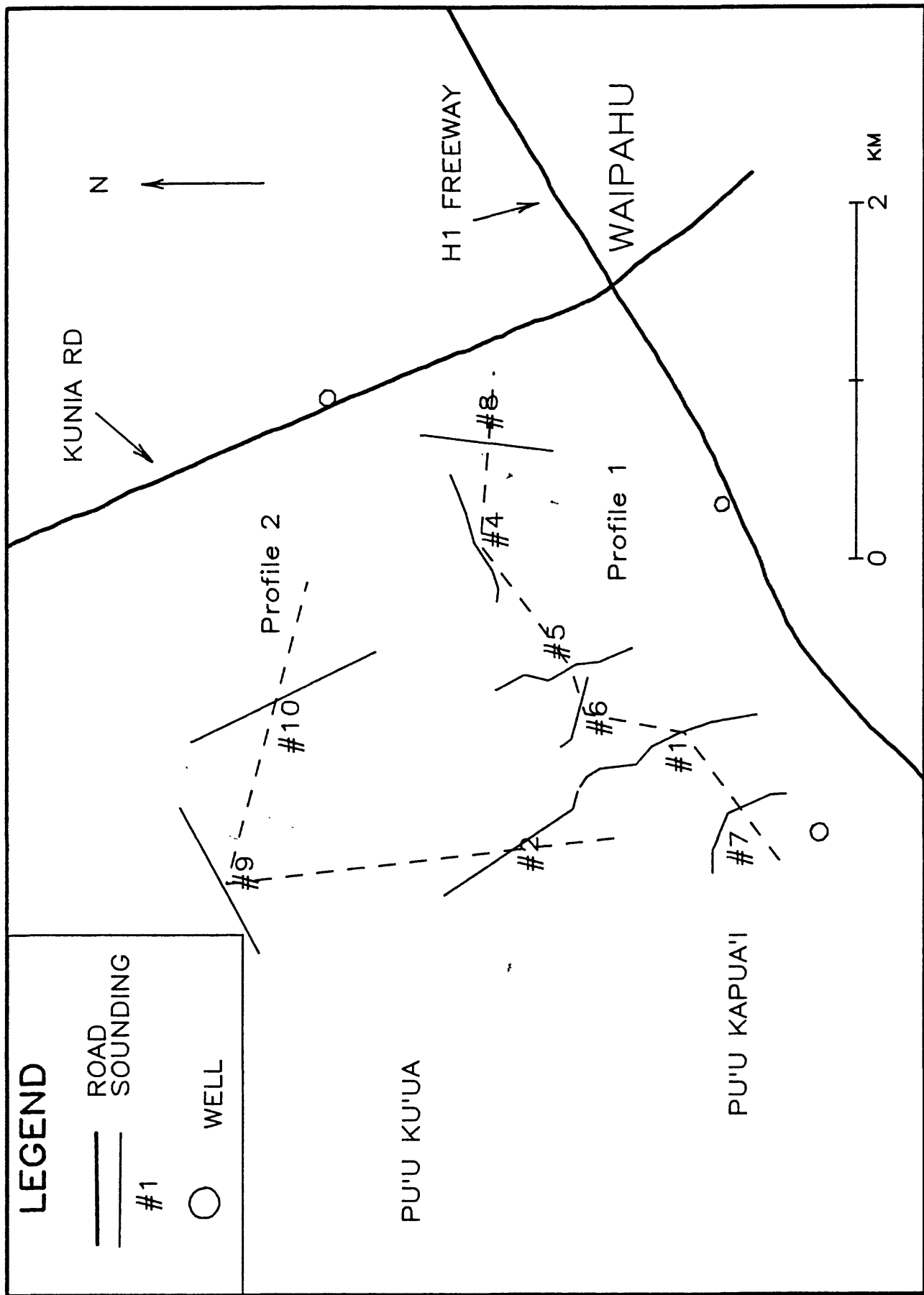


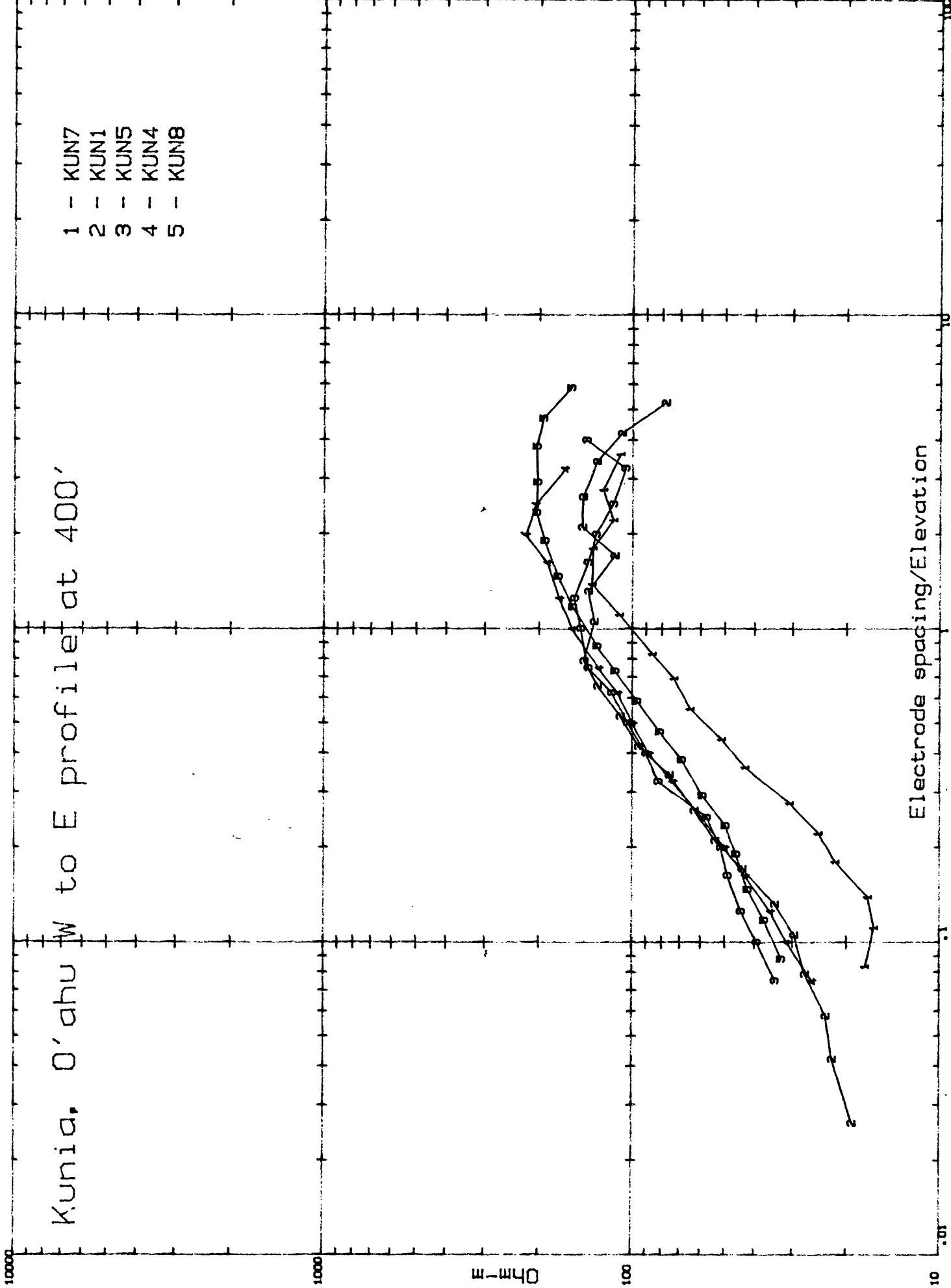
Fig. 3



Fig. 4

Kunia, O'ahu W to E profile at 400'

- 1 - KUN7
- 2 - KUN1
- 3 - KUN5
- 4 - KUN4
- 5 - KUN8



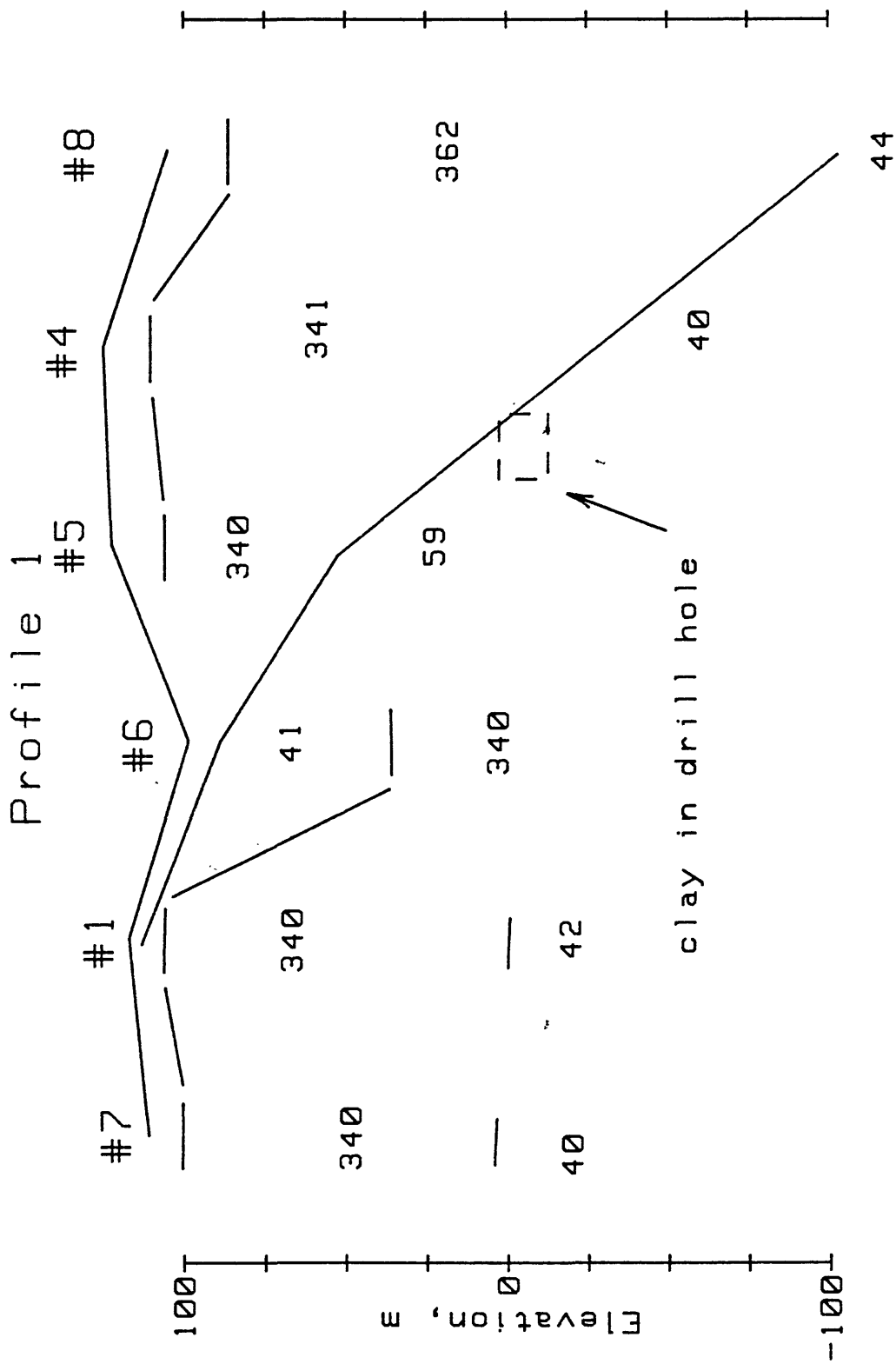


Figure 5 (horizontal distances not to scale)

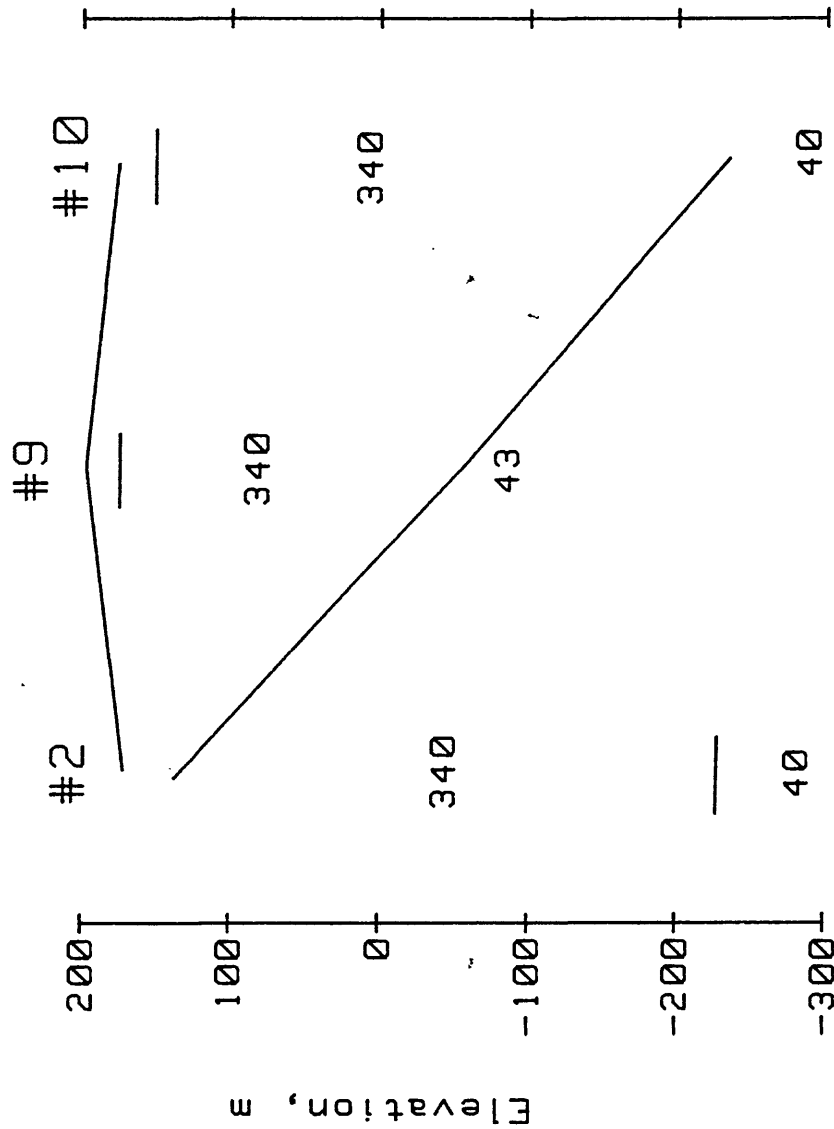


Figure 6 (horizontal distances are not to scale)

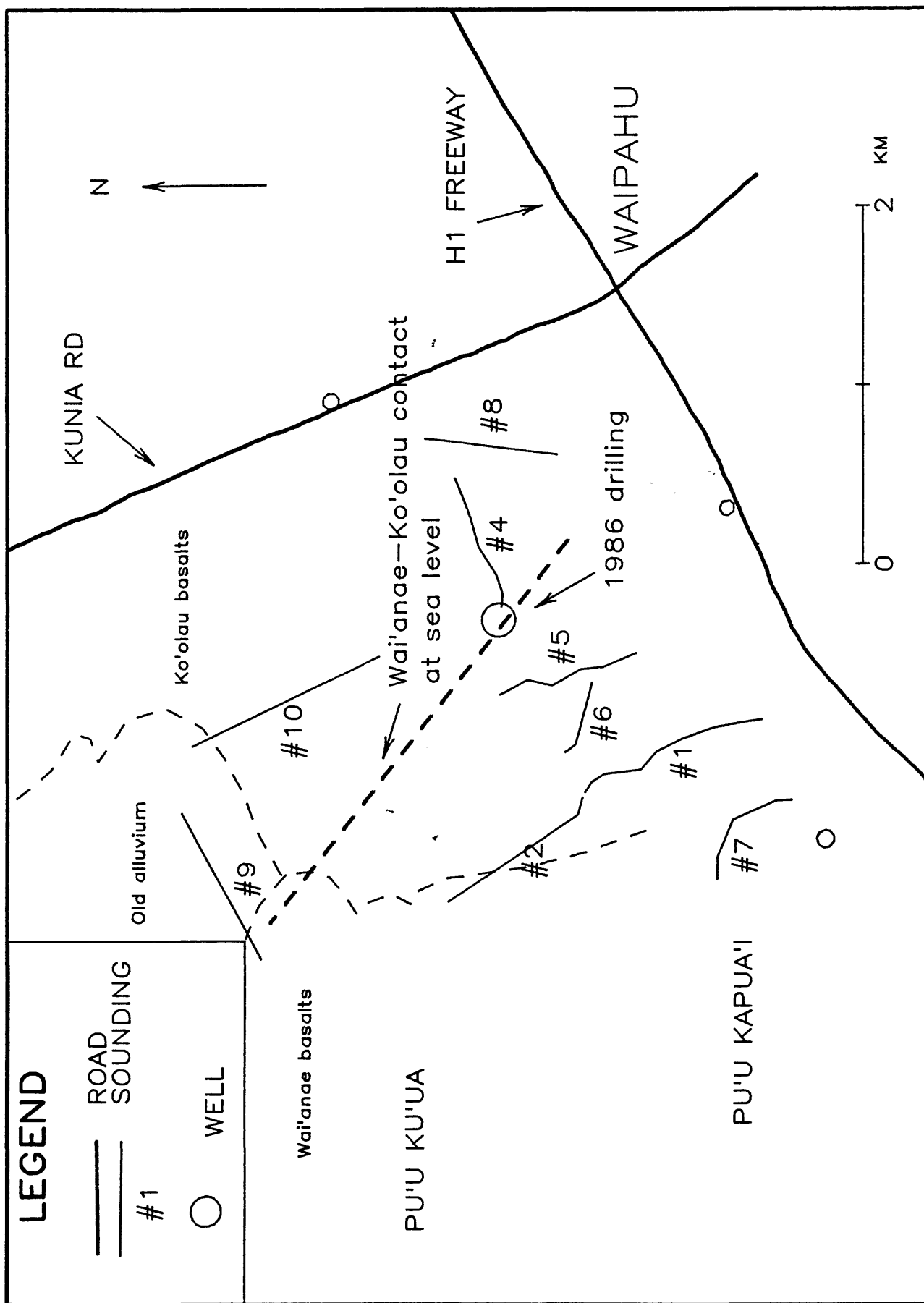


Fig. 7

## REFERENCES

- Anderson, W. A., 1979, Program MARQDCLAG -- Marquardt inversion of Dc-Schlumberger soundings by lagged-convolution: U.S. Geological Survey Open-File Report 79-1432, 58 p.
- Kauahikaua, J. and Shettigara, V., 1984, Electrical resistivity investigation of the Schofield high-level water body, Oahu, Hawai'i: U.S. Geological Survey Open-File Report 84-646, 27 p.
- Stearns, H.T., and Vaksvik, K.N., 1935, Geology and Groundwater Resources of the island of Oahu, Hawaii: Div. of Hydrography, Bull. 1, 479 p.
- Visher, F.N. and Mink, J.F., 1964, Ground-water resources of southern Oahu, Hawaii, USGS WSP 1778, 133 p.